

April 1, 2005

RD42 Collaboration
contact: P. Weilhammer
CERN, EP-Division
1211 Geneve 23
e-mail: Peter.Weilhammer@cern.ch
Fax: (41)-22-767-7150
Tel: (41)-22-767-5817

Element Six LTD - Diamond Division
King's Ride Park
Ascot
Berkshire SL5 8BP
England
Tel: +44-1344-638200 (switchboard)
Fax: +44-1344-638236

Report on Samples, No. 1/2005

Abstract

This report contains the following items

- LHCC Referee's Report on RD42 Activities
- Comparison of charge collection measurements
- Recent irradiation studies
- Discussion of thinning of DBDS-91,92
- New results on scCVD diamonds
- BaBar/Belle/CDF/ATLAS results with pCVD material
- Discussion of wafer samples and processing

1 LHCC Referees Report

The RD42 results for 2004 were presented to the LHC Committee (LHCC) on 2-Feb-2005. The referee's report was submitted to the LHCC on 28-Feb-2005 in LHC document CERN/LHCC 2005-004 LHC 74. Below we present the minutes of the LHC 28-Feb meeting and referee's report on RD42 activities (extracted from CERN/LHCC 2005-004):

REPORT FROM THE RD42 REFEREE

The LHCC heard a report from the RD42 referee on the collaboration's programme concerning the development of intrinsically radiation-hard Chemical Vapour Deposition (CVD) diamond devices.

Good progress was reported for the past year. In particular, improvements were reported on the charge collection distance of polycrystalline CVD (pCVD) diamond and good results were shown on the response, charge versus sensor thickness and the transient current measurements been made on single crystal CVD (scCVD) diamond. The Committee also took note of the continuing development of diamond pixel detectors and of applications to beam monitoring and beam abort systems for collider experiments.

The LHCC considers that the proposed research programme for 2005, concentrating on the construction and test of diamond pixel detector modules with the ATLAS and CMS front-end electronic chips, the characterization of higher quality scCVD, continuation of irradiation tests and test of the beam condition monitors for use in collider experiments such as ATLAS and CMS, to be reasonable.

In view of the above and given the modest request for resources for further work, the referee recommends that the R&D project be continued in 2005. A status report is expected to be submitted to the LHCC in one year's time. The Committee agrees to the continuation of the project on this basis.

2 Charge Collection Measurements and FWHM (CD samples)

These measurements were done in the PUMPED state

Diamond	t	d-OSU	d-CERN	d-UT	MP(e)	FWHM(e)	FWHM/MP
CD65	520	170@1.0	169@+1.	142@1.0	4100	4500	1.12
		161@1.0	160@-1.		4100	4500	1.12
CD66	525	167@1.0	157@+1.	151@1.0	4000	4200	1.05
		159@1.0	135@-1.		4000	4100	1.03
CD67	525	167@1.0	155@+1.	147@1.0	4000	4125	1.03
		154@1.0	150@-1.		4000	4050	1.01
CD68	520	178@1.0	159@+1.	184@1.0	4400	4125	0.94
		168@1.0	151@-1.		4200	4125	0.98
CD69	520	183@1.0	156@+1.	155@1.0	4250	4275	1.01
		166@1.0	138@-1.		4000	4125	0.98
CD70	525	167@1.0			4100	4075	0.99
		163@1.0			4100	4200	1.02
CD71	520	173@1.0			--	--	--
		162@1.0			3900	3925	1.01
CD72	520	182@1.0			--	--	--
		172@1.0			3900	3925	1.01
CD75	520	171@1.0		90@1.0			
		182@1.0					
CD76	520	186@1.0		140@1.0			
		177@1.0		136@1.0			
CD77	520	166@1.0		119@0.8			
		174@1.0		130@0.8			
CD78	520	167@1.0		146@1.0			
		158@1.0					
CD79	520	151@1.0			3400	3300	0.97
		120@1.0			3000	3000	1.00
CD80	440	140@1.0			3000	3300	1.10
		125@1.0			2900	3000	1.03
CD81a	515	230@1.0					
		212@1.0					
CD81b	515	213@0.8					
		197@1.0					

CD81c	515	216@1.0 175@1.0				
CD85	500	209@1.0 199@1.0		5000 5000	5000 5000	1.00 1.00
CD86	500	191@1.0 199@1.0		5500 4800	5200 4800	0.95 1.00
CD87	500	207@1.0 203@1.0	233@+1. (e)	5100 5100	4900 4900	0.96 0.96
CD88	500	196@1.0 207@1.0		5200 5000	5200 5000	1.00 1.00
CD89	490	204@1.0				
CD92	470	204@1.0 196@1.0		5500 5500	5600 5600	1.02 1.02

CD99	490	134@1.0 76@1.0				
CD100	470	143@1.0 100@1.0				
CD101	470	122@1.0 70@1.0				
CD102	480	132@1.0				
CD103	470	117@1.0				
CD104	470	122@1.0				

CD109	490	220@1.0 230@1.0	243@+1. (e) 247@+1.	6720 6900	6200 6800	0.93 0.99
			262@-1. (h) 264@-1.	8000 7440	7440 7400	0.93 1.00
CD110	480	204@1.0 200@1.0	220@+1. (e) 239@+1. 255@-1 (h) 267@-1.	5790 6820 7840 7040		
CD111	490	215@1.0 220@1.0	252@+1. (e) 253@+1. 261@-1. (h) 263@-1.	7140 6220 7920 7200		
CD112	490	225@1.0 225@1.0				

CD113	490	225@1.0	174@+1. (e)	
		228@1.0	210@-1. (h)	
CD114	490	245@1.0	257@+1. (e)	7440
		230@1.0	260@+1	7500
			272@-1. (h)	7650
			275@-1.	7630

CD116	490	221@1.0	252@+1. (e)	5500	5900
		223@1.0		5500	5900

Comments:

In "good diamonds" the charge signal begins at >1500e.

In "good diamonds" the FWHM/MP < ~1.2.

3 Charge Collection Measurements and FWHM (UT samples)

These measurements were done in the PUMPED state

Diamond	t	d-OSU	d-CERN	d-UT	MP(e)	FWHM(e)	FWHM/MP
UTS5	432	184@1.0		202@1.0			
			191@1.0		6000	6600	1.10
UTS6	480	173@1.0	195@1.0		4000	4350	1.09
		164@1.0			4000	4350	1.09
UTS8	480	182@1.0	193@1.0	217@1.0	4650	5000	1.08
		167@1.0					
UTS9	470	185@1.0	178@1.0	148@1.0	4400	5000	1.14
		165@1.0			3900	4650	1.19
UTS13-1	615	199@1.0					
		194@1.0					
UTS13-4	615	194@0.8					
		198@0.8					
UTS14-1	555	120@0.9					
UTS14-2	555	182@1.0					
		170@0.9					
UTS14-3	550	183@1.0					
		183@1.0					
UTS14-4	550	112@0.7					
		75@0.3					
UTS14-5	550	129@0.9					
		135@0.7					
UTS15	470	89@0.8		-	B,L,P		
UTS16	470	93@0.8		-	B,L,P		
UTS17	470	73@0.8		-	B,L,P		
UTS20	510	123@1.0			2500	2800	1.12
UTS21	510	155@1.0					
UTS22	510	150@1.0					
UT23-P1e	540	168@1.0					
UT24-P1e							
UTS25	480	195@1.0			5000	5400	1.08
		180@1.0			4700	4800	1.02

UTS26	470	203@1.0	5000	5400	1.08
		202@1.0	5000	4700	0.94
UTS27	490	191@1.0	4800	5300	1.10
		193@1.0			
UTS28	480	177@1.0	4700	4300	0.91
		204@1.0	5300	5900	1.11
UTS29	490	195@1.0	4600	5600	1.22
		176@1.0	4100	4700	1.14
UTS30	480	197@1.0	5400	5700	1.06
		178@1.0	4500	4400	0.98

Comments:

In "good diamonds" the charge signal begins at >1500e.

In "good diamonds" the FWHM/MP < ~1.2.

4 Comparison of Measurements - OSU, CERN, Rutgers

The updated table below shows a comparison of the collection distance of recent CD samples (CD109, 110, 111, 112, 113, 114, 116 and for comparison CD87) measured at CERN, OSU and Rutgers. These are the samples from the latest polycrystalline runs. The measurements were performed using a ^{90}Sr β -source.

These measurements were done in the PUMPED state

Diamond	t	d-CERN	d-OSU	d-Rutgers
CD109	490	243@+1.0 (e) 247@+1.0 262@-1.0 (h) 264@-1.0	220@+1.0 230@+1.0	
CD110	480	220@+1.0 (e) 239@+1.0 255@-1.0 (h) 267@-1.0	204@+1.0 200@+1.0	178@1.0 189@1.0
CD111	490	252@+1.0 (e) 253@+1.0 261@-1.0 (h) 263@-1.0	215@+1.0 220@+1.0	
CD112	490		225@+1.0 225@+1.0	
CD113	490	174@+1.0 (e) 210@-1.0 (h)	225@+1.0 228@+1.0	
CD114	490	257@+1.0 (e) 260@+1.0 272@-1.0 (h) 275@-1.0	245@+1.0 230@+1.0	215@1.0
CD116	490	252@+1.0 (e)	221@+1.0 223@+1.0	195@1.0
CD87(o)	500		207@+1.0 203@+1.0	
CD87(n)	500	233@+1.0 (e)	210@+1.0 199@+1.0	215@1.0

5 Irradiation Studies of Recent Samples

Earlier RD42 proton irradiation studies indicated that pCVD diamond trackers are radiation tolerant up to a fluence of 2.2×10^{15} p/cm². These results are shown in Fig. 1.

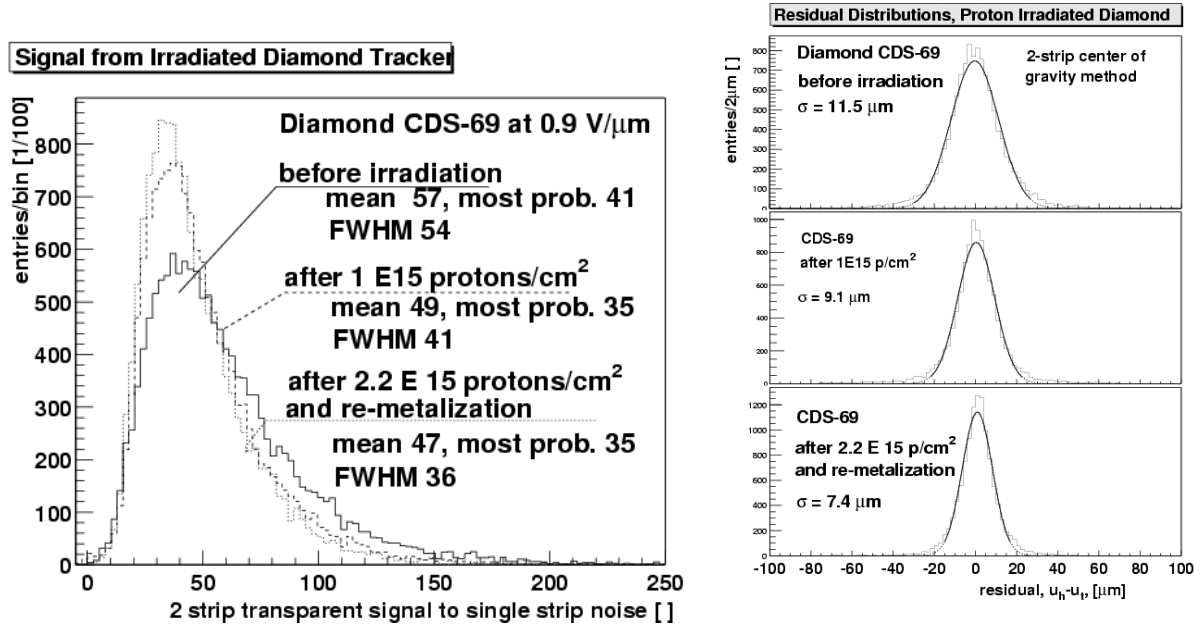


Figure 1: Charge signal distribution and tracking residual for CD69 before proton irradiation, after 1×10^{15} p/cm² and after 2.2×10^{15} p/cm².

In order to update and extend these results with higher quality diamonds we have started an irradiation with pCVD diamond CD113. CD113 was irradiated in Oct. 2004 up to a fluence of 2×10^{16} p/cm². This figure corresponds to a dose of roughly 500Mrad. CD113 was also tested in the Nov. 2004 CERN testbeam as a strip detector. In Fig. 2 we show the pulse height distribution before and after the irradiation to 20×10^{15} p/cm². At this fluence the pCVD diamond retains 25% of its original pulse height.

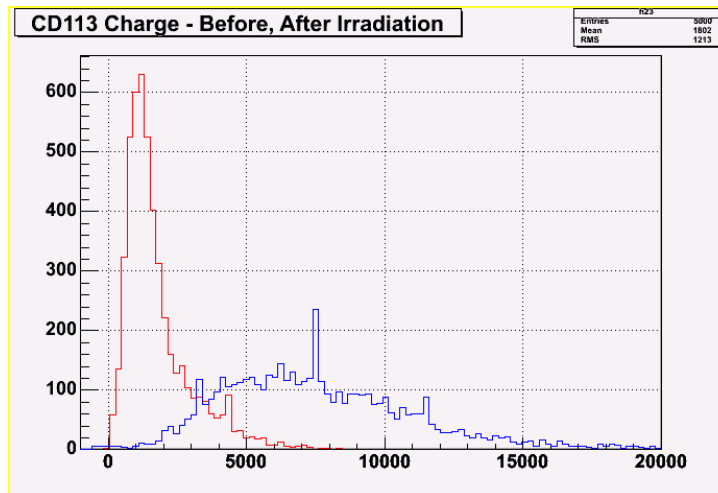


Figure 2: Pulse height distributions before (blue curve) and after (red curve) the irradiation of CD113 to 20×10^{15} p/cm².

In Fig. 3 we show a summary of the proton irradiation results described above. We find that all of the irradiations fall along an exponential curve. The diamond signal is down by $1/e$ at 12.5×10^{15} p/cm². In Fig. 3 we also show the results of the first irradiation of any scCVD diamond. Our preliminary data indicates that scCVD diamond is damaged more easily than pCVD material. These results are in the process of being checked.

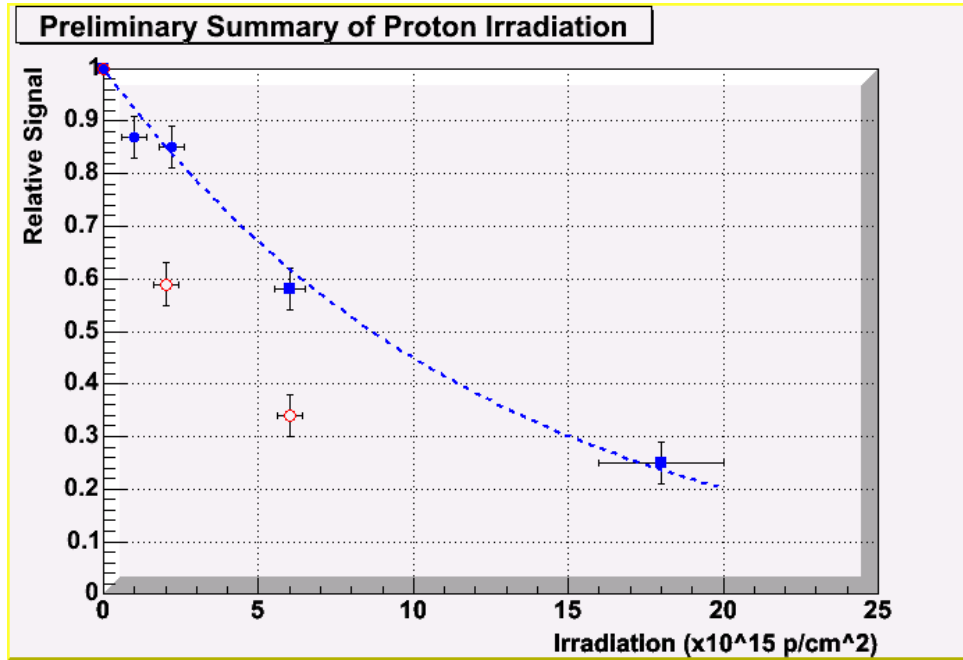


Figure 3: Summary of proton irradiation results for pCVD material up to a fluence of 20×10^{15} p/cm² (filled data points). The blue curve is an exponential with exponent $-0.08 \times \text{fluence}$ indicating a radiation lifetime for this material of 12.5×10^{15} p/cm². Also shown are the results of the irradiation of the first scCVD diamond (open data points).

6 Material Removal from Samples DBDS-91,92

The samples DBDS-91 and DBDS-92 were used to study the consequences of material removal on the charge signal. Originally the samples were metalized at DeBeers. Using these contacts the samples showed polarization. At OSU the contacts were removed and cleaned, O₂ plasma etched and remetalized. Cr/Au electrodes were placed on both sides of each sample and charge collection data were taken. The samples were then sent to other centers for measurement and on to DeBeers for material removal. After material removal one electrode remained on each sample and looked (visually) fine but it was removed. The samples were cleaned and O₂ plasma etched. The new Cr/Au contacts were placed on the both samples. The samples were re-measured and the process repeated. The results are as follows:

```
Results: DB-91  Original thickness 800 um
                marked side up data ccd=188 um
                marked side dn data ccd=151 um

                After first material removal thickness = 660 um
                marked side up data ccd=154 um
                marked side dn data ccd=132 um

                After second material removal thickness = 590 um
                marked side up data ccd=136 um
                marked side dn data ccd=119 um

                After third material removal thickness = 460 um
                marked side up data ccd=111 um
                marked side dn data ccd=105 um

                After fourth material removal thickness = 360 um
                marked side up data ccd= 81 um
                marked side dn data ccd= 58 um

                After fifth material removal thickness = 300 um
                marked side up data ccd= 63 um
                marked side dn data ccd= 48 um

                After sixth material removal thickness = 260 um
                marked side up data ccd= 51 um
                marked side dn data ccd= 33 um

                After seventh material removal thickness = 200 um
                marked side up data ccd= 41 um
                marked side dn data ccd= 33 um

                After eighth material removal thickness = 97 um
                marked side up data ccd= 16 um
                marked side dn data ccd= 15 um
```

Results: DB-92 Original thickness 780 um
marked side up data ccd=144 um
marked side dn data ccd=180 um

After first material removal thickness = 610 um
marked side up data ccd=156 um
marked side dn data ccd=188 um

After second material removal thickness = 560 um
marked side up data ccd=189
marked side dn data ccd=206

After third material removal thickness = 450 um
marked side up data ccd=181 um
marked side dn data ccd=172 um

After fourth material removal thickness = 320 um
marked side up data ccd=120 um
marked side dn data ccd=158 um

After fifth material removal thickness = 290 um
marked side up data ccd=107 um
marked side dn data ccd=124 um

After sixth material removal thickness = 260 um
marked side up data ccd=107 um
marked side dn data ccd=123 um

After seventh material removal thickness = 200 um
marked side up data ccd=101 um
marked side dn data ccd=118 um

After eighth material removal thickness = 142 um
marked side up data ccd= 91 um
marked side dn data ccd= 97 um

After ninth material removal thickness = 85 um
marked side up data ccd= 68 um
marked side dn data ccd= 67 um

Fig. 4 shows distributions from the material removal experiment. Material removal from the growth side (red) follows a linear relationship. Material removal from the substrate first rises then falls. The falling curve, however is not limited by the thickness of the material (dotted blue line) and intersects the material thickness limit at around $65 \mu\text{m}$ collection distance indicating that one carrier is trapped at roughly this distance.

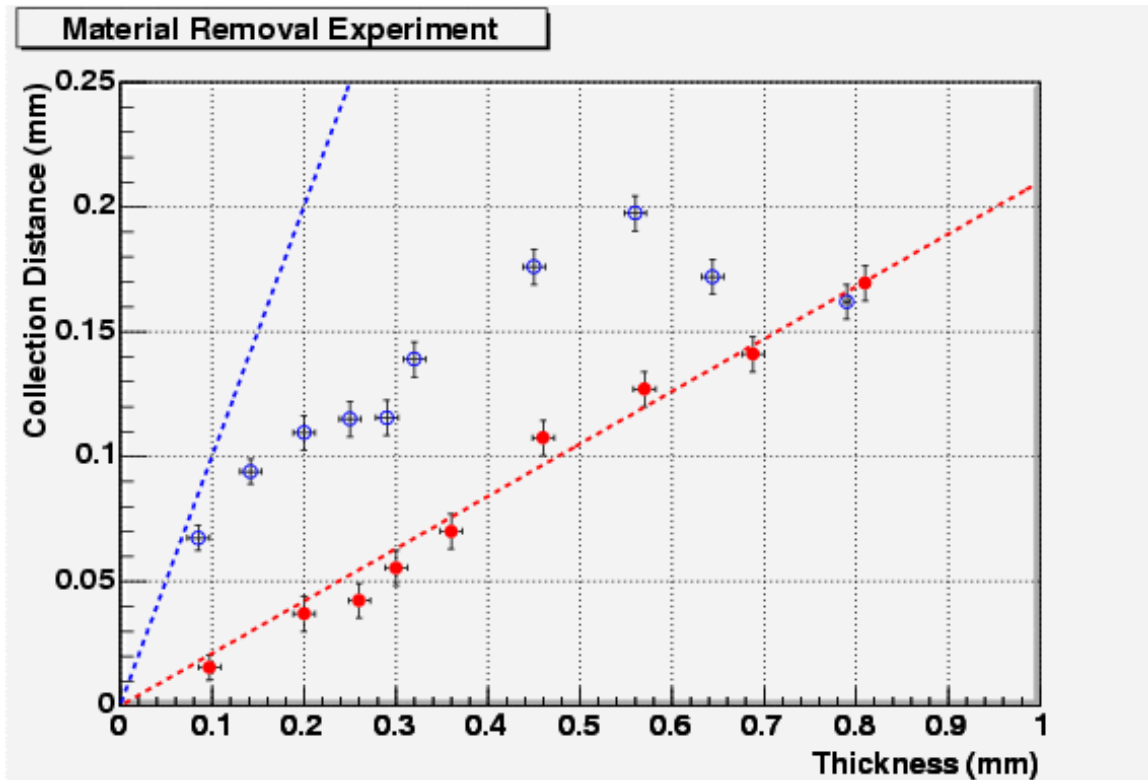


Figure 4: Collection distance from the thinning samples DB-91 and DB-92.

7 Results on Single Crystal CVD Diamonds

The data below indicates 4 classes of scCVD diamond.

7.1 Charge Collection Measurements and FWHM

Diamond	t		d-OSU	d-CERN	MP(e)	FWHM(e)	FWHM/MP
071415	450	e	440@+1.0	564@+1.0	17500	5200	0.30
		h		556@-1.0	17890	5500	0.31
		e	433@+1.0	547@+0.5	17400	5580	0.32
		h		544@-0.6	17400	5600	0.32
CD-135	440	e	420@+1.0		13750	4000	0.29
		h					
		e	430@+1.0		13600	3750	0.28
		h					
CD-135(r)	440	e	443@+1.0				
		h					
		e	443@+1.0				
		h					
CD-135(r')	440	e	444@+1.0				
		h					
		e	448@+1.0				
		h					
CD-135(m)	330	e	82@+0.6				
CD-135(m')	330	e	65@+1.0				
CD-135(m'')	330	e	95@+1.0				
CD-135(m''')	330	e	324@+1.0		9600	3200	0.33
CD-140	455	e	164@+0.2				
		e	29@+0.1				
CD-140(r)	440	e	388@+0.5				
		e	360@+0.1				

170301	471	e	401@+0.3	486@+0.4	16650	8600	0.52
		h		467@-0.4	15550	8060	0.52
		e		451@+0.4	15050	8060	0.54
		h		479@-0.4	15640	8510	0.54
CD-127	430	e	407@+0.7				
		h					
		e	404@+0.7				
		h					
CD-127(m)	425	e	136@+0.1				
CD-127(m')	425	e	304@+0.4				
		e	216@+0.1				
CD-134	490	e	430@+0.6				

		h		
		e	424@+0.6	
		h		
CD-134(m)	470	e	76@+0.4	
CD-134(m')	470	e	110@+0.8	
CD-134(m'')	470	e	115@+0.8	
CD-134(m''')	470	e	340@+0.4	
CD-134(m''''')	470	e	420@+0.4	
CD-134(m''''''')	470	e	435@+0.8	
		e	430@+0.6	
CD-134(m''''''''')	470	e	472@+1.0	323@0.4
		h		355@0.4
		e	430@+0.6	
CD-137	350	e	292@+1.0	
		h		
		e	298@+1.0	
		h		
CD-137(m)	350	e	303@+1.0	

170320	690	e	645@+1.0	
		h		248@-1.0
		e	200@+1.0	
		h		
CD-136	840	e	305@+1.0	
		h		
		e	211@+1.0	
		h		
CD-138	365	e	274@+1.0	
		h		
		e	* I problem	
		h		
CD-138(m)	365	e	358@+0.8	
		e	80@+0.8	
CD-139	380	e	93@+0.3	
		h		
		e	* I problem	
		h		
CD-139(m)	380	e	103@+0.3	
		e	202@+0.8	

91302c	380	e	81@+1.0*	
		h		
		e	63@+1.0*	
		h		
91302d	390	e	43@+1.0*	
		h		

e 71@+1.0*
h

Notes:

First pair of measurements are with dot-ring side up; second pair dot-ring down.

Comments:

In Si the FWHM/MP = ~0.5.

In Si the charge distribution begins at 75% of the MP charge.

Si does not exhibit pumping.

Problems:

170301 breaks down @0.4V/umdefects visible on one surface.
CD-127 draws 20 nA @0.7V/umno defects visible.
CD-134 draws 20 nA @0.8V/umno defects visible.
CD-136 draws 3/3 nA @1.0V/umno defects visible.
CD-137 draws 3/3 nA @1.0V/umno defects visible.
CD-138 draws 1/20 nA @0.3V/umno defects visible.

7.2 Charge Distributions

In Fig. 5 and Fig. 6 we show the pulse height spectrum observed from four single crystal CVD diamonds. The diamonds are 210 (CD168), 330 (CD135), 450 (071415), and 685 μm thick (CD141). We observe collection distances consistent with full charge collection; most probable charges of 5,500e, 9,500e, 13,400e and 22,500e; FWHM's of 3000e, 3000e, 4000e, and 8000e; and more than 4,000e, 7,000e, 10,000e and 15,000e separation between the pedestal and the beginning of the charge distribution. The FWHM/MP for these single crystal CVD diamonds is approximately 0.3-0.5, about one third that of polycrystalline CVD diamond and about two thirds that of correspondingly thick silicon.

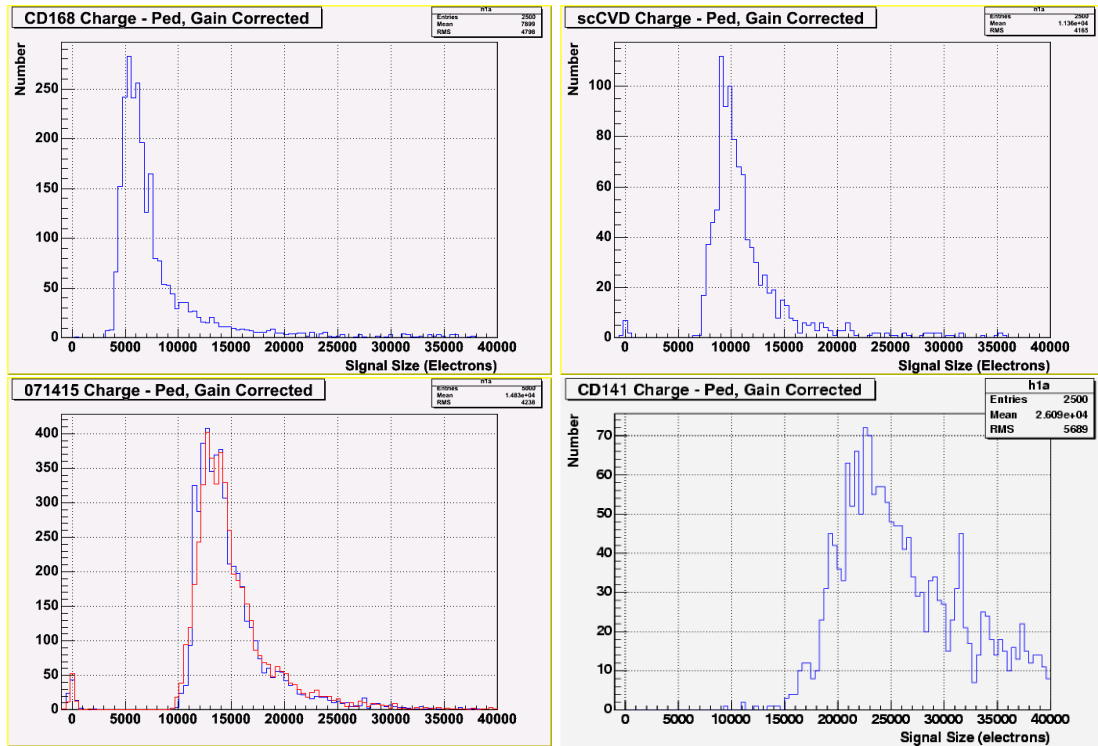


Figure 5: The pulse height distribution of scCVD diamonds. The thicknesses of the diamonds are, from top left to to bottom right, 210 (CD168), 330 (CD135), 450 (071415), 685 μm (CD141). When there are two curves they are the results for positive and negative applied voltage.

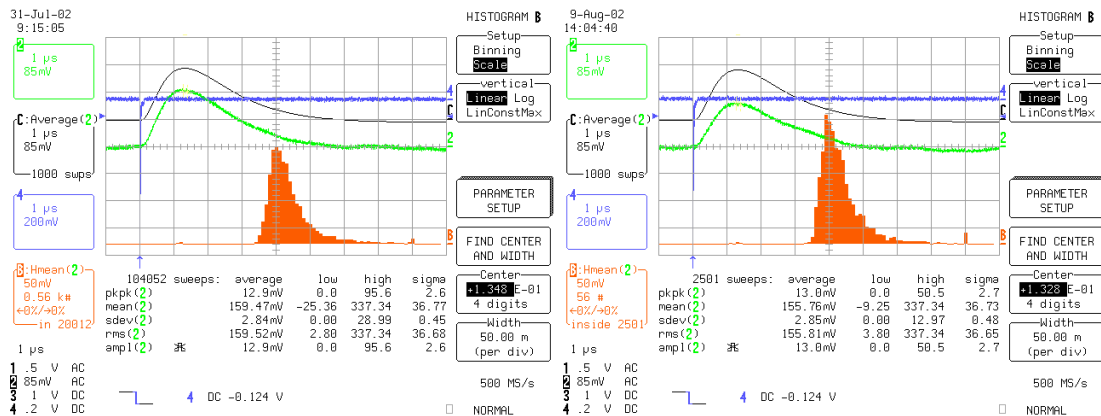


Figure 6: CERN measured charge distribution from recent scCVD sample 071415 for holes from the dot side (upper) and holes from the back side (lower).

In Fig. 7 we show the most probable charge for scCVD diamond versus thickness of the material. A clear linear relationship is evident out to thicknesses of $770 \mu\text{m}$. As with silicon, thinner samples have less charge per unit thickness than thicker samples.

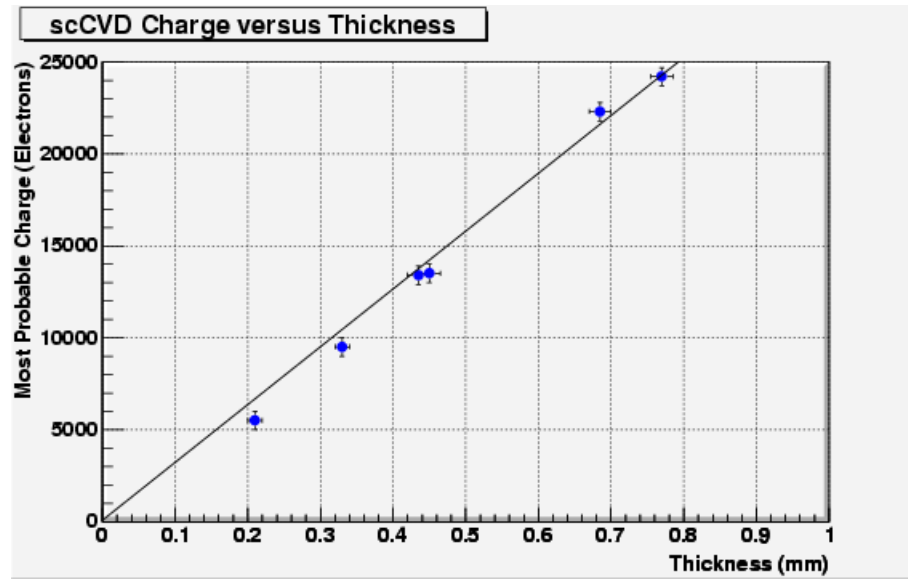


Figure 7: The most probable pulse height versus thickness for scCVD diamonds.

7.3 HV Properties

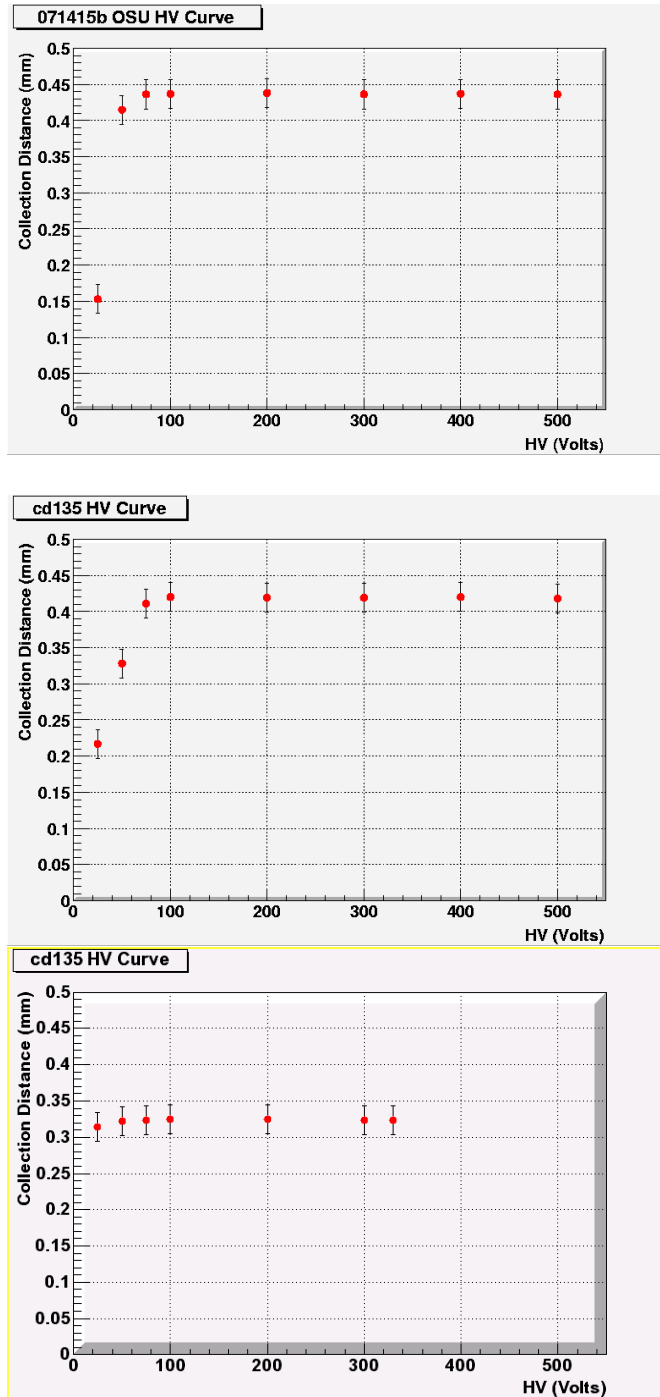


Figure 8: HV curve for scCVD samples 071415b ($t=450\mu\text{m}$), CD135 ($t=440\mu\text{m}$) and CD135 ($t=330\mu\text{m}$) indicating that full charge is collected at $<100\text{V}$ (an applied electric field of $0.2\text{V}/\mu\text{m}$).

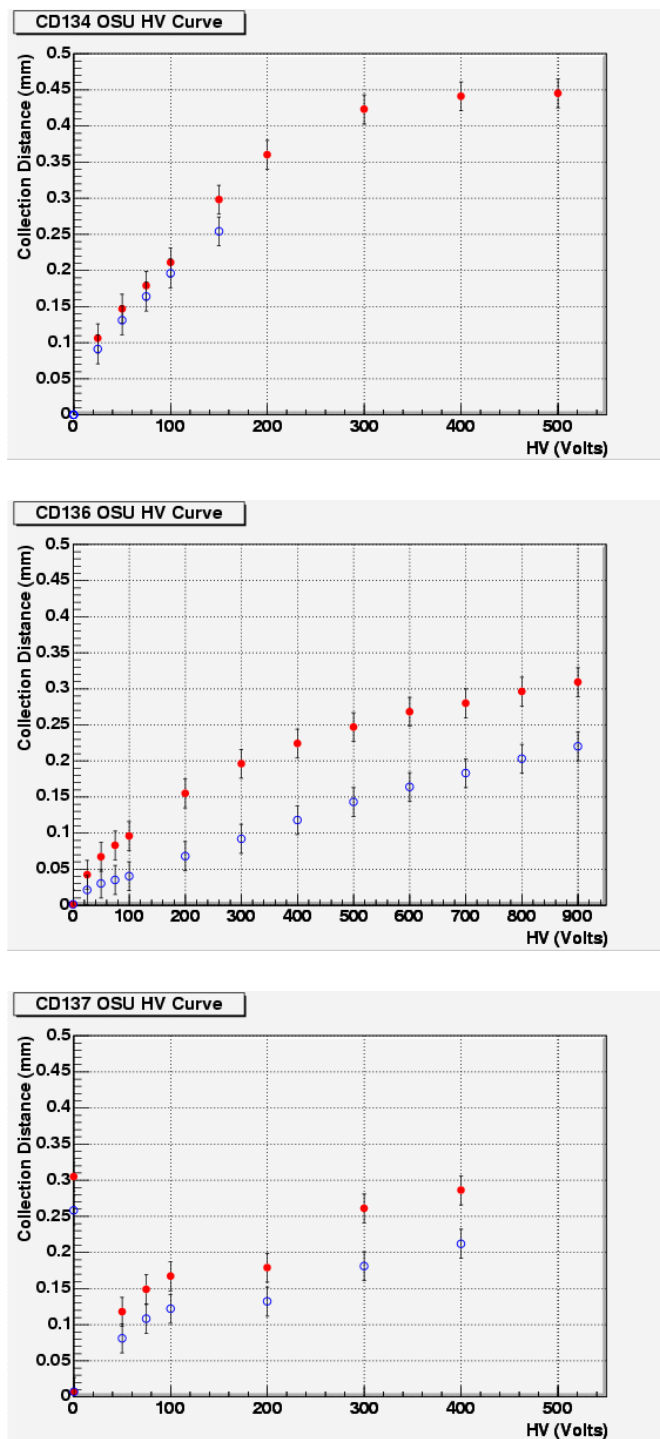


Figure 9: HV curve for scCVD samples CD134, CD136 ($t = 840\mu\text{m}$) and CD137 ($t=350\mu\text{m}$).

7.4 Pumping Properties

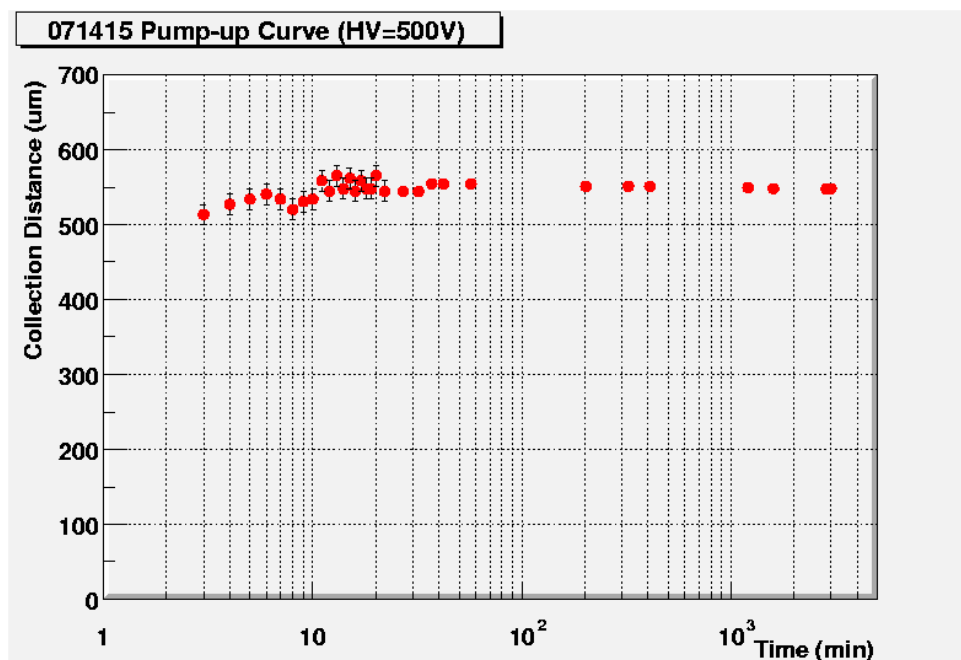


Figure 10: Time dependence of charge signal from scCVD sample 071415.

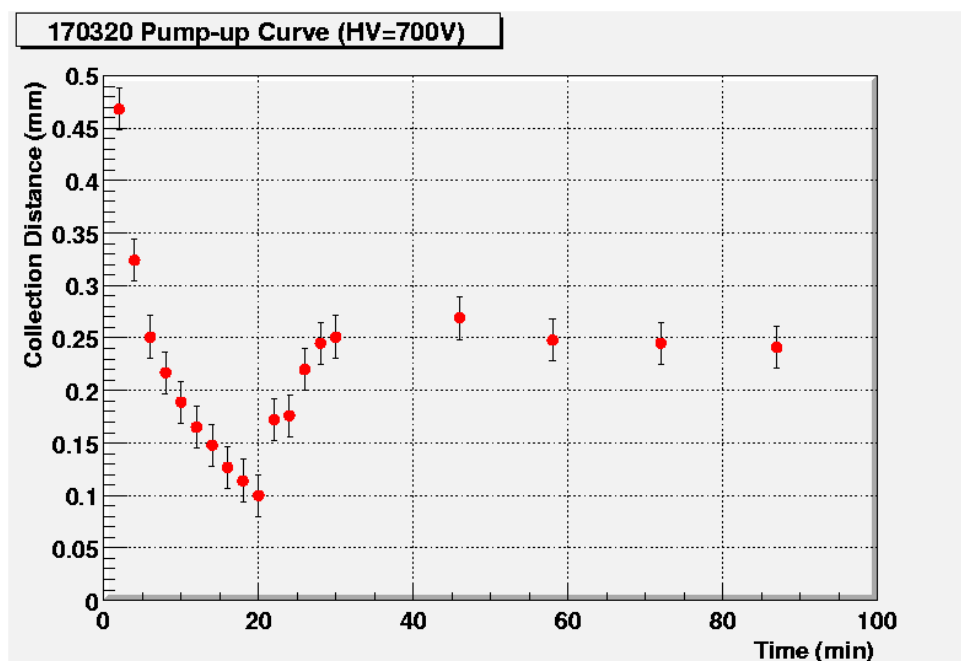


Figure 11: Time dependence of charge signal from scCVD sample 170320.

7.5 Research Contract

The scCVD diamonds CD-140, 141, 142, 143 were developed as part of the scCVD research contract. CD140 is the physically the largest and measures $\approx 7\text{mm} \times 7\text{mm}$. Each of these diamonds has a different surface finish. Photographs of the diamonds are shown below:

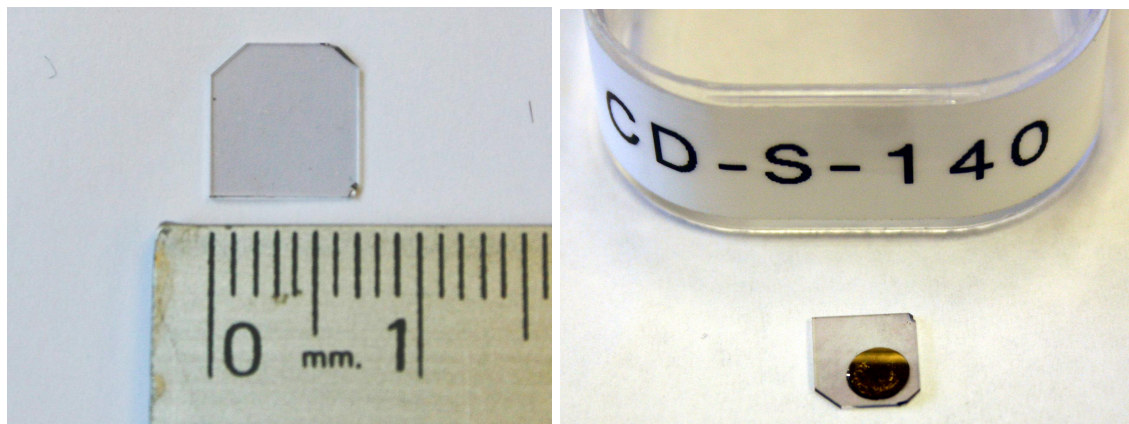


Figure 12: Photographs of CD140.

The data from these samples is shown below:

Name	area	thickness	ccd@E
CD140	7.70mmx7.30mm	455um	164@0.220/ 29@0.111
CD140(r)		440um	388@0.455/360@0.114
CD141	5.50mmx5.10mm	690um	608@0.694/347@0.278 <-- OSU 143
CD141(m)			685@0.571/664@0.571
CD142	5.85mmx5.14mm	600um	330@0.132/326@0.132
CD143	4.80mmx4.53mm	770um	771@0.909/650@0.520 <-- OSU 141



Figure 13: Photos of the surface of scCVD samples CD141, CD142 and CD143.

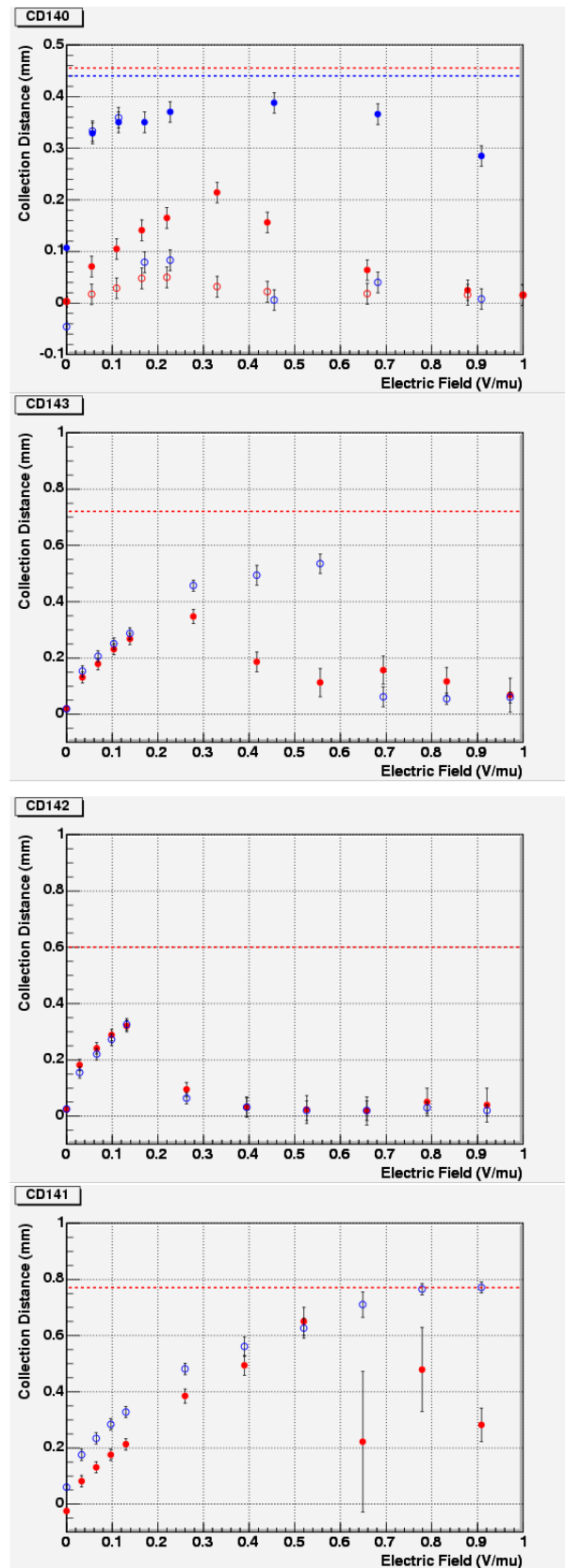


Figure 14: HV curves for scCVD samples CD140 before and after material removal, CD141, CD142, and CD143.

The scCVD diamonds CD-140, 166, 167, 168 were delivered parts of the scCVD research contract.

Name	area	thickness	ccd@E
CD166		610um	344@0.984/372@0.984
CD167	8.25x10.15	575um	560@0.174/560@0.174
CD168		210um	201@0.954/202@0.954

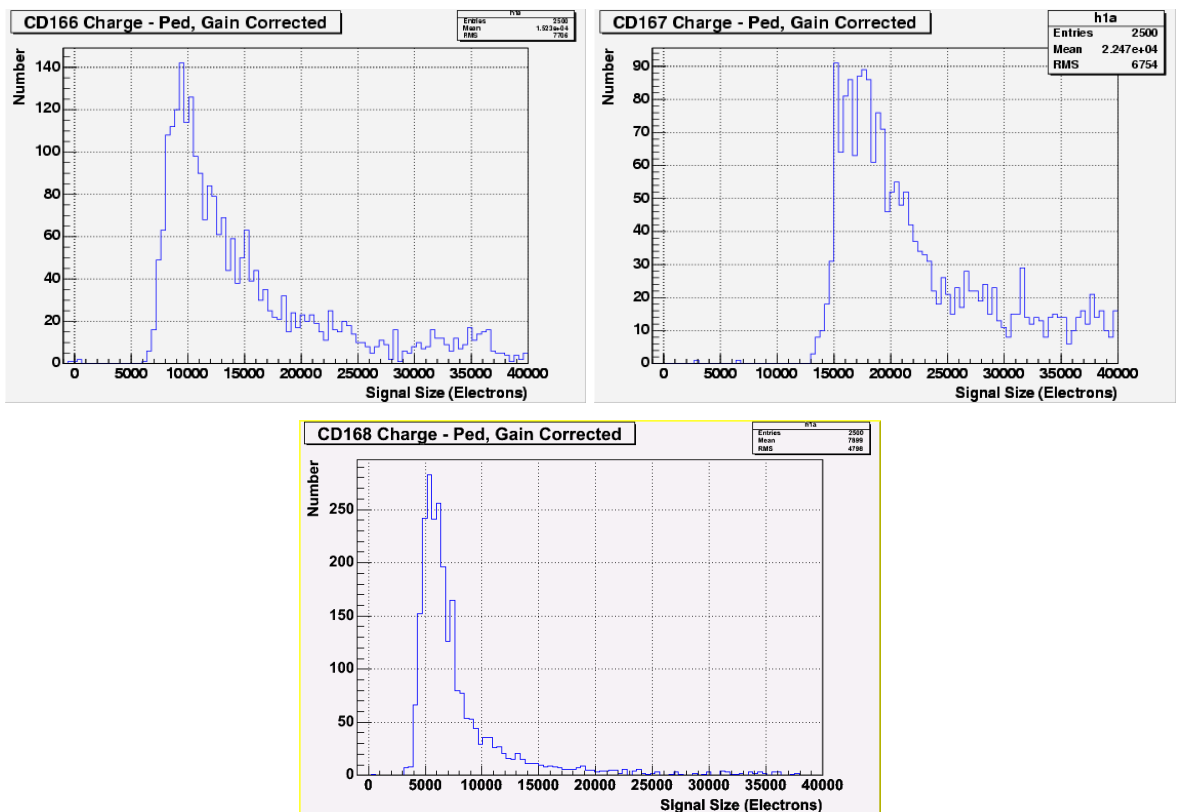


Figure 15: Pulse height distributions for scCVD samples CD166, CD167 and CD168 at $E=0.984V/\mu\text{m}$, $0.174V/\mu\text{m}$, and $0.954V/\mu\text{m}$

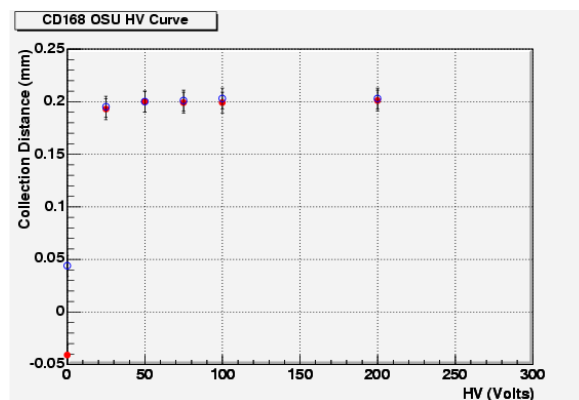


Figure 16: HV curve for CD168.

7.6 Irradiation Studies of scCVD Sample 071415

Diamond	t		d-OSU	d-CERN	MP(e)	FWHM(e)	FWHM/MP
071415	450	e	440@+1.0	564@+1.0	17500	5200	0.30
		h		556@-1.0	17890	5500	0.31
		e	433@+1.0	547@+0.5	17400	5580	0.32
		h		544@-0.6	17400	5600	0.32
071415-Irrad	450	e	216@+1.0	<-- after 2×10^{15} sample now pumps			
		e	257@+2.0				
		h					
		e					
071415-Irrad	450	h					
		e	103@+1.0				
		e	150@+2.0				
		h					
		e					
		h					

Notes:

First pair of measurements are with dot-ring side up; second pair dot-ring down.

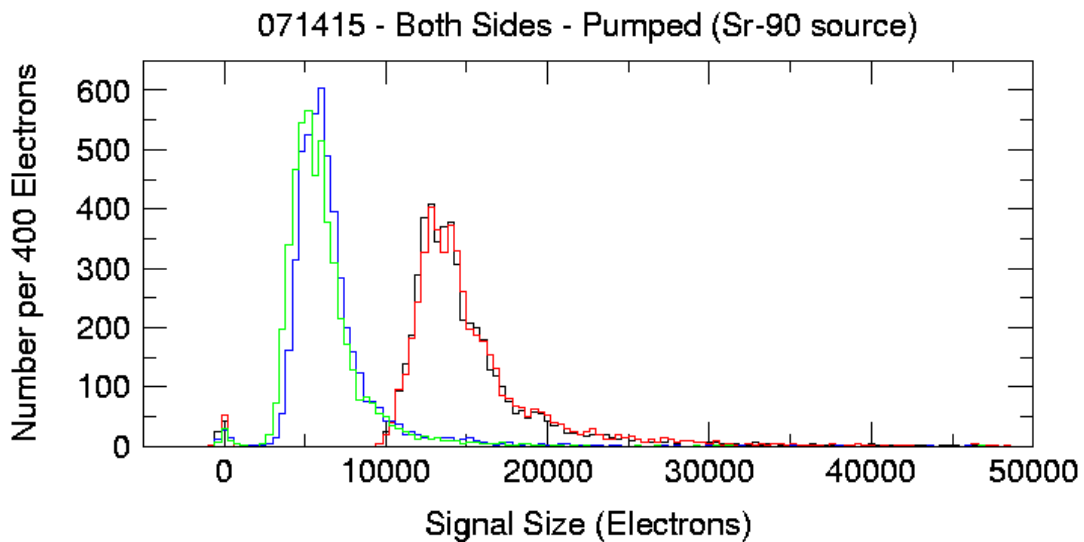


Figure 17: Pulse Height spectrum of scCVD sample 071415 before and after irradiation with 2×10^{15} protons/cm².

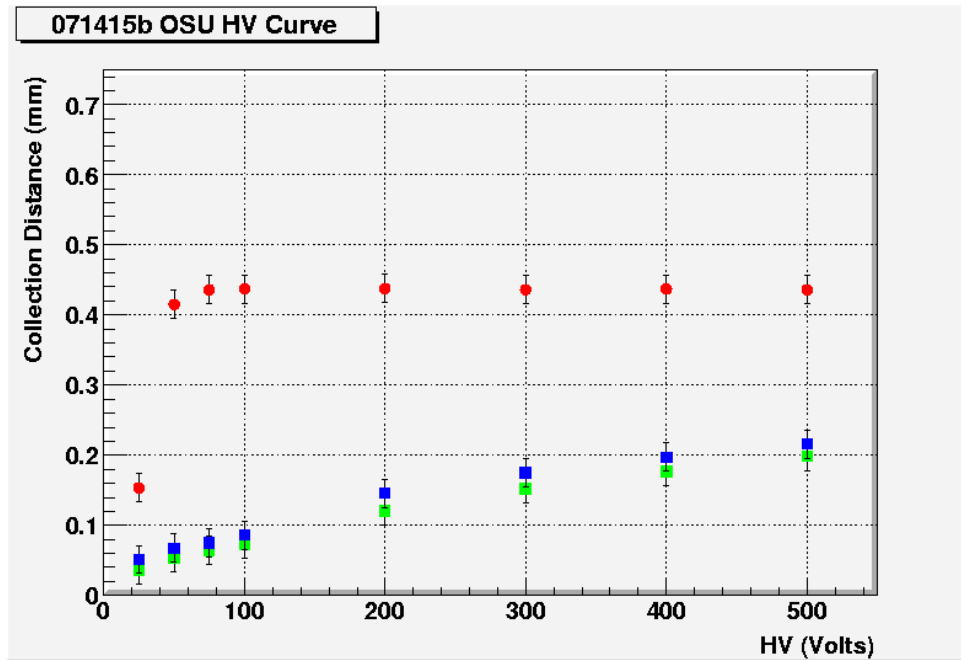


Figure 18: Collection distance of scCVD sample 071415 before and after irradiation with 2×10^{15} protons/cm².

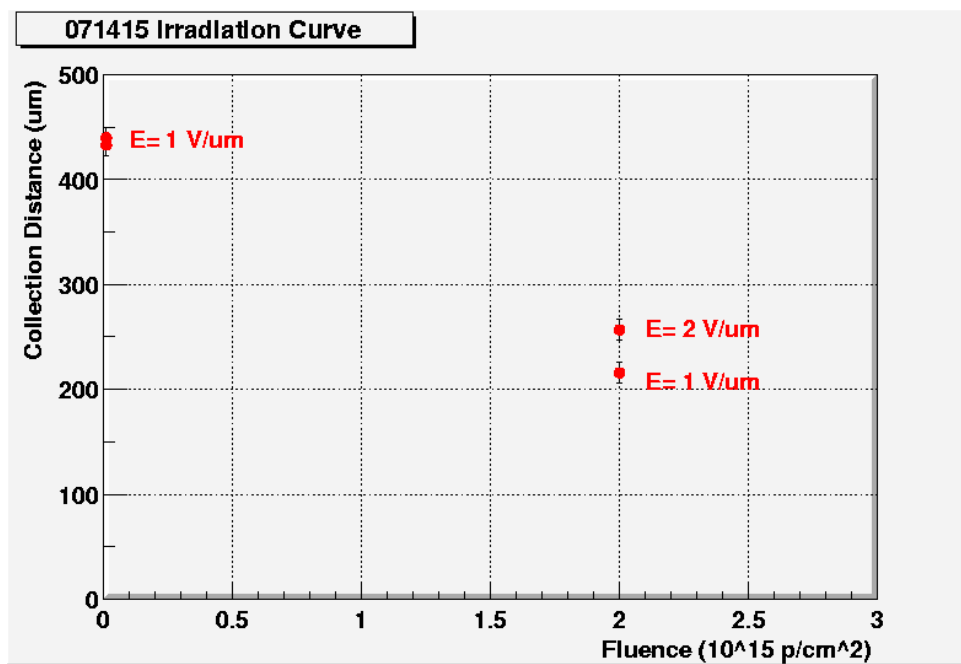


Figure 19: Proton irradiation summary with scCVD sample 071415.

8 BaBar/Belle Diamond SVTRad Status in pCVD diamond

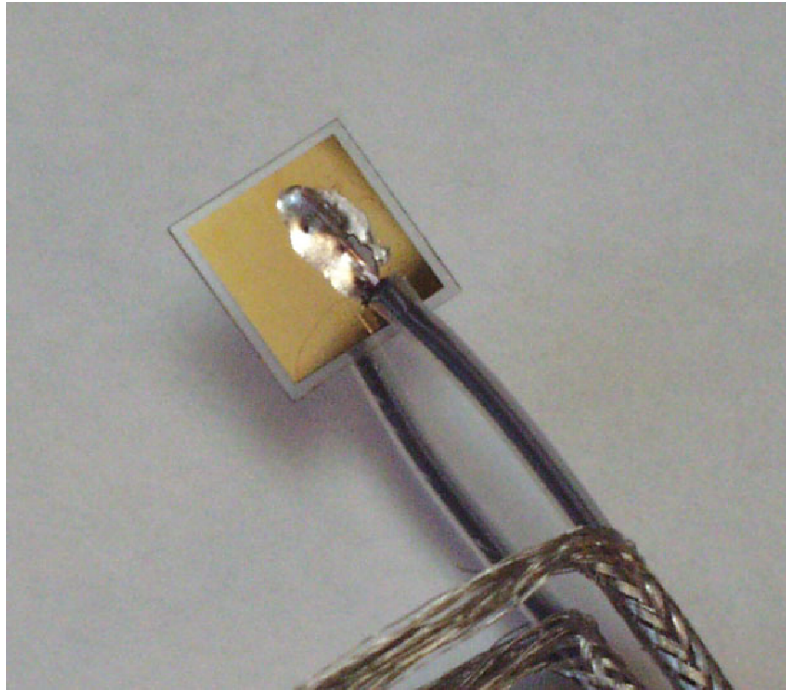


Figure 20: Polycrystalline CVD samples prepared for BaBar SVT monitoring.

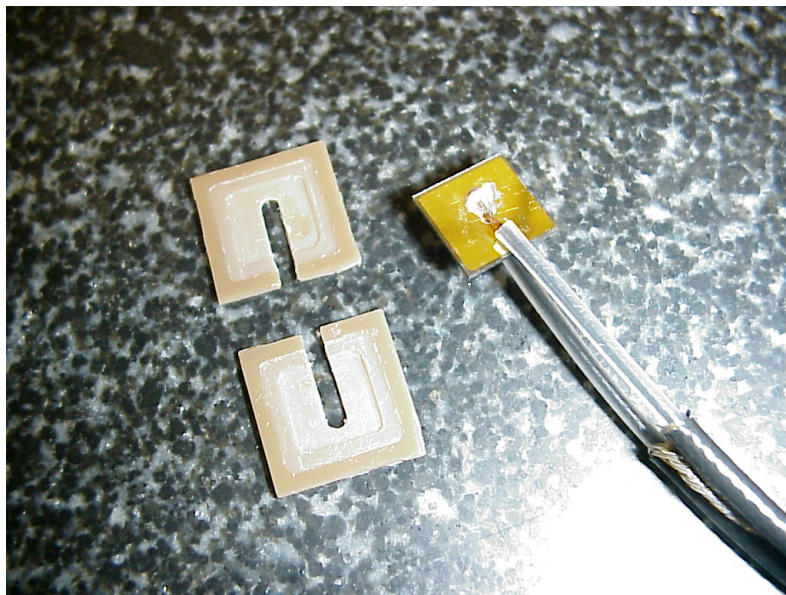


Figure 21: Polycrystalline CVD samples prepared for Belle SVT monitoring.

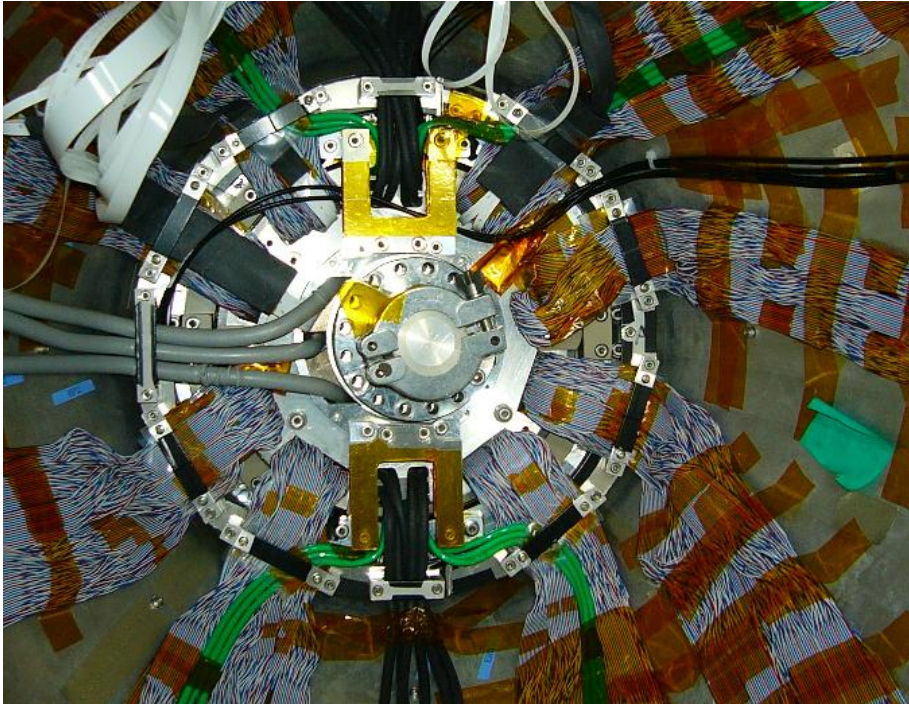
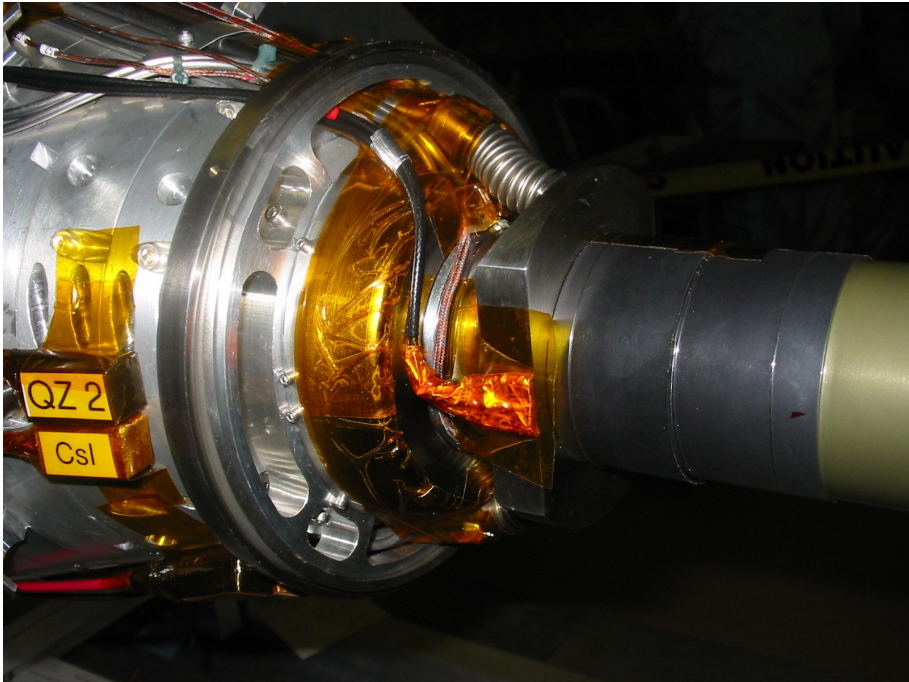


Figure 22: Photo of installed BaBar and Belle devices.

The Belle Diamond Radiation Monitor Program:

First beam has been seen with the diamond beam monitors installed in the Belle experiment in August of 2003 (see photos in figs 21 and 22). The diamond data with relatively slow sampling time correlate well with silicon PIN diodes that are the main-stay of the BELLE background monitoring system.

A fast amplifier (shaping time 50ns) was also used to study signals from the diamond sensors installed at BELLE. Figures 23 and 24 show scope traces of output from this fast amplifier that were triggered on a silicon PIN diode during an abort of the KEK B factory beam. In the first figure (50 μ s per division) one sees the rise of the silicon PIN diode in the lower trace and the response of the diamond in the upper trace. Figure 24 shows another abort, where now the response of the silicon diode is barely visible on the 1 μ s timescale, while the diamond signal is limited by the readout electronics showing a rise-time of less than 100 ns. These tests revealed some impedance mismatches in the readout that resulted in ringing with a time-constant of about 500ns – seen as the ripples that follow the diamond pulse. These problems have now been resolved.

The readout electronics used at BELLE are being upgraded to improve the signal to noise for the slowly shaped signal. The cabling that connects the diamonds to the amplifier will be re-done late this summer to reduce (hopefully eliminate) impedance mismatches so that we can further study the fast time response of the diamond monitors.

Figure 25 and Fig. 26 shows the silicon and diamond beam monitors during a beam instability. This event was NOT observed in the silicon monitors and is clearly visible in the diamond monitor.

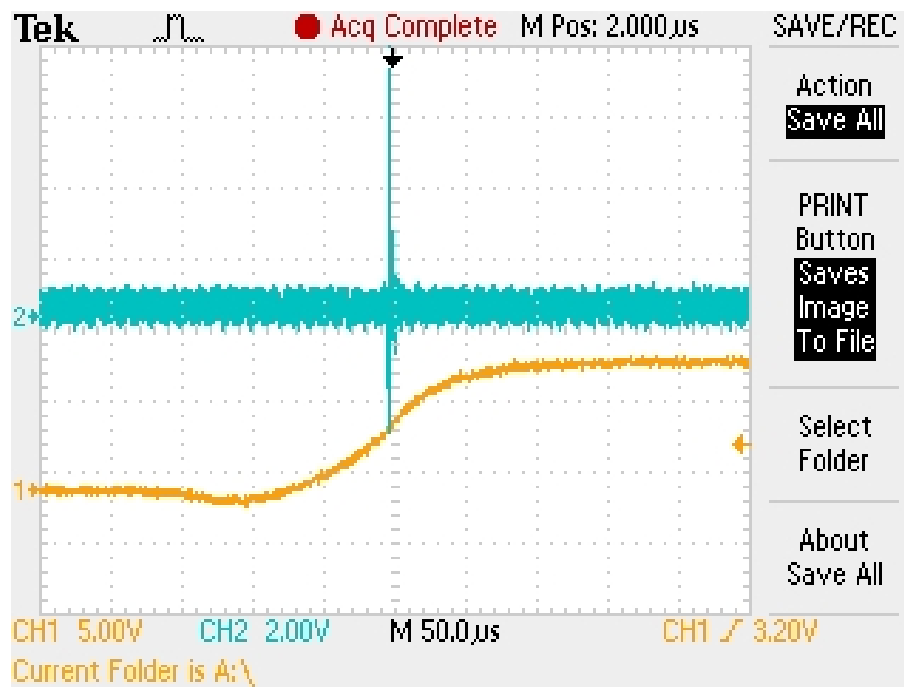


Figure 23: The response of the diamond beam monitor (upper trace) to a beam abort in the KEK B factory accelerator complex, when triggered by a silicon PIN diode (lower trace).

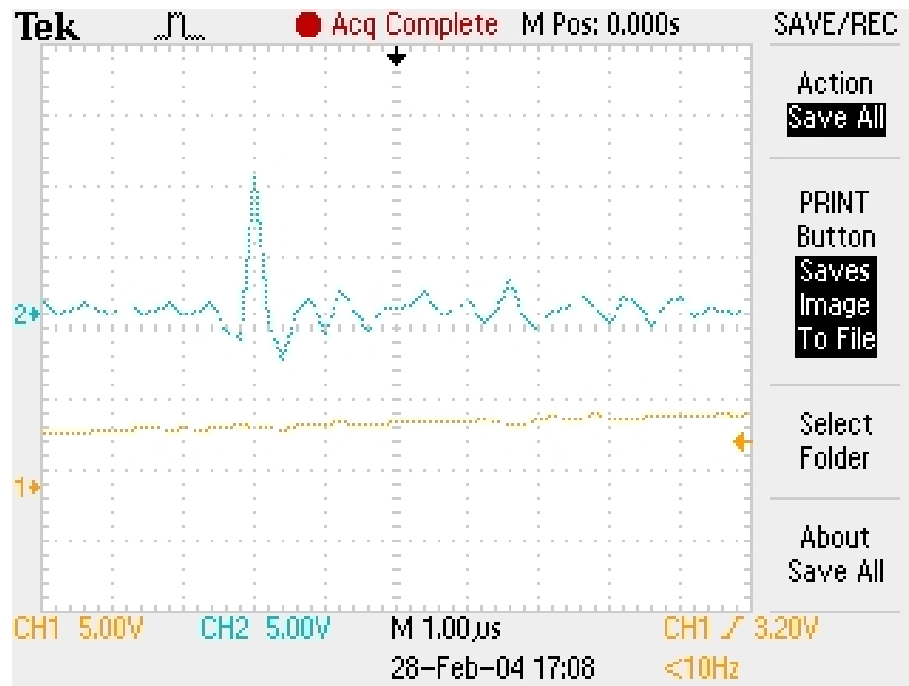


Figure 24: The response to a similar beam abort over a much shorter time interval. Now the response of the silicon is barely perceptible while the diamond signal rise is limited by the readout amplifier.

The QCS (Superconducting final focus quadruple) magnet quenched and MOSFET/PIN diode response.

- A terrible beam instability happened and beam entered QCS on Sep 14, 2004 at 18:02. QCS quenched after the beam is lost.
- Belle suffered from 2 krad at a moment. Fortunately, Belle SVD is working well.
- There were no beam abort request from Belle/SVD.
- SVD PIN monitor showed no response at 18:02.
- Further investigation is done.

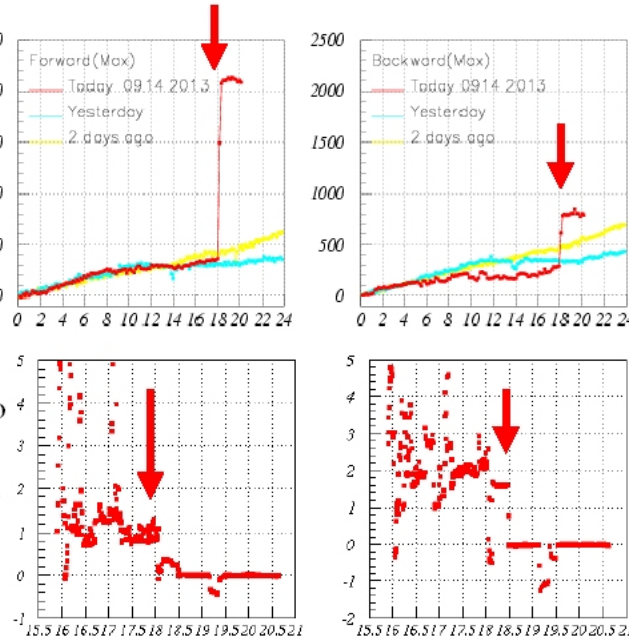


Figure 25: The response of the silicon during a magnet quench leading to a beam instability.

Response of CVD diamond radiation sensors

- CVD diamond sensors are put at the IP chamber entrance. We have been thinking they have much lower gain than PIN diodes. However, for this time, the result was excellent.
- Both ADCs for Dia1 and Dia2 overflowed. *Dia1* and *Dia2* showed at least 10 and 50 time, respectively, larger signal than the usual radiation level.
- A 1-sec RC low-pass filter is inserted in front of ADC. The signal could be much much more larger, had we not adopted such a filter. (Anyway, the ADC range was 0.1V max).

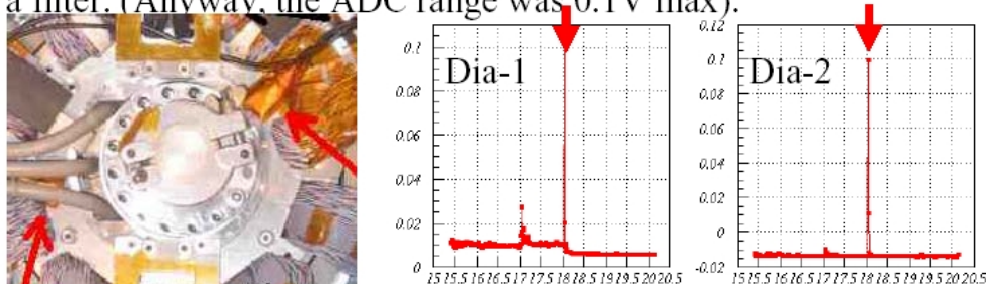


Figure 26: The response of the diamond during a magnet quench leading to a beam instability.

The K2K Neutrino Generation Beam Monitoring:

The K2K experiment in Japan produces an intense neutrino beam in Eastern Japan and detectors them in the large underground water Cherekov experiment in the Japanese Alps, 245 km to the west. These neutrinos are produced from the decay of pions at the Accelerator at KEK. In order to understand and optimize the neutrino production mechanisms the K2K experiment would like a beam monitor that can withstand the intense pion fluxes required.

They have studied the use of a simple diamond sensor in the pion beam during running in the fall of 2003. Here we show a scope trace showing the diamond pulse height from the 9 pion bunches, spaced approximately 150 ns apart. Here the diamond is readout without an amplifier. The beam intensity is such that the several volt signals shown come directly to the oscilloscope on about 20m of cable.

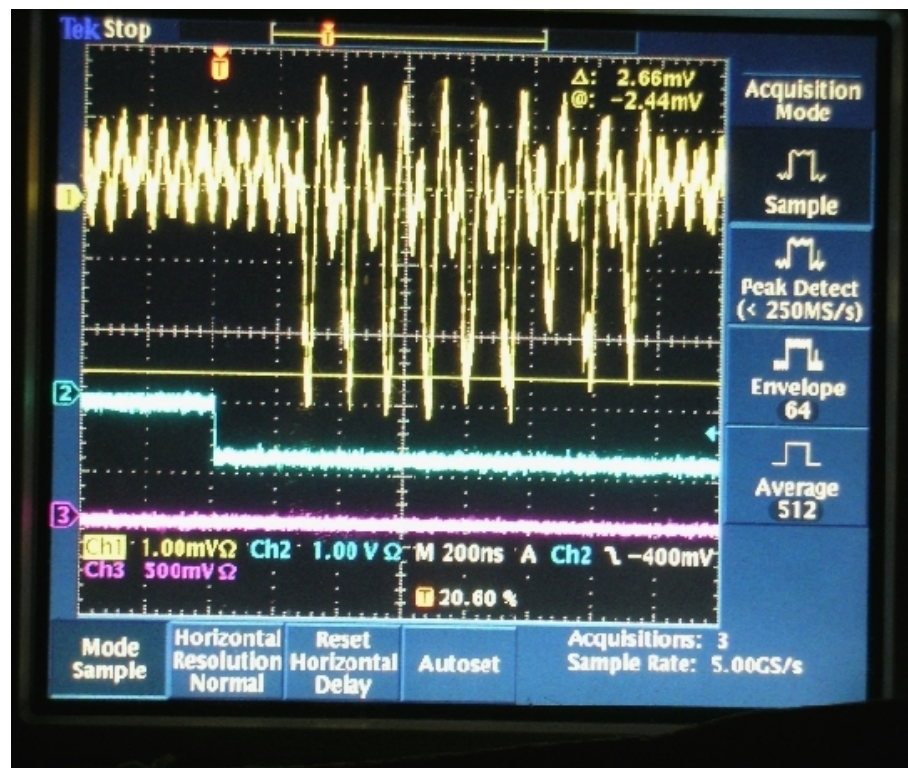


Figure 27: Pulses from nine successive bunches of pions producing a neutrino beam for the K2K experiment in Japan.

There will be one last run of the K2K experiment this fall where these studies will continue, but the R&D is aiming at a larger system for the next generation Japanese Neutrino Oscillation experiment (T2K) that is scheduled to be taking data at the end of this decade. That experiment will use a much more intense pion source (from the Tokai accelerator – now under construction just north of the current HEP lab in Japan).

The CDF Diamond Radiation Monitor Program:

During the Fall 2004 shutdown CDF installed one diamond to test as a radiation monitor. The CDF experiment has already had many beam incidents that have caused failures in its silicon detector. During the last year of data taking alone CDF reports it lost or damaged 2.5% of all SVXII chips due to beam incidents. As this is the closest environment to the LHC it was decided to install a diamond to see how it performs.

A photograph of this device is shown in 28 and a picture of the installation is shown in 29. The present radiation monitoring system of CDF relies on measuring the ever increasing leakage current in silicon diodes. The diamond will provide the first real-time measurement of radiation inside the CDF detector. The diamond has been observed to have a background leakage current of $\approx 5\text{pA}$. The diamond has recently observed its first beams as the Fermilab Tevatron is starting operation.

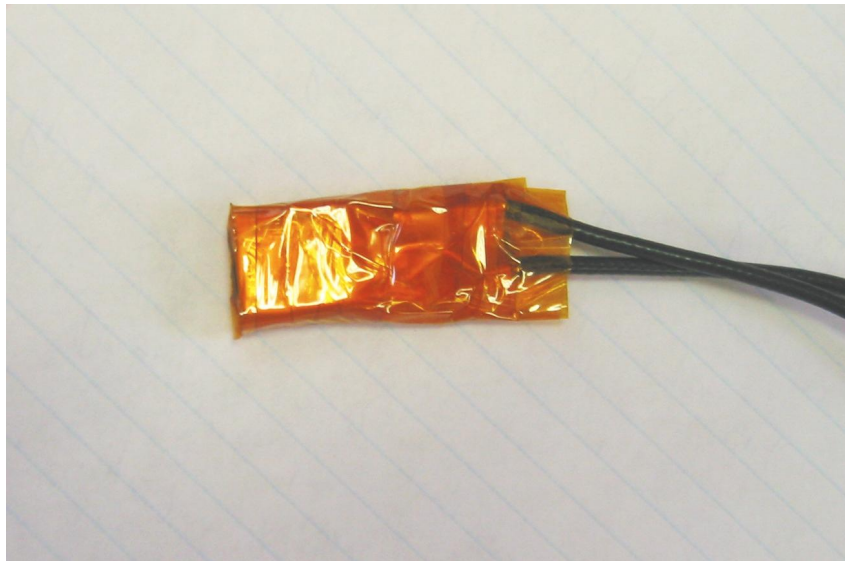
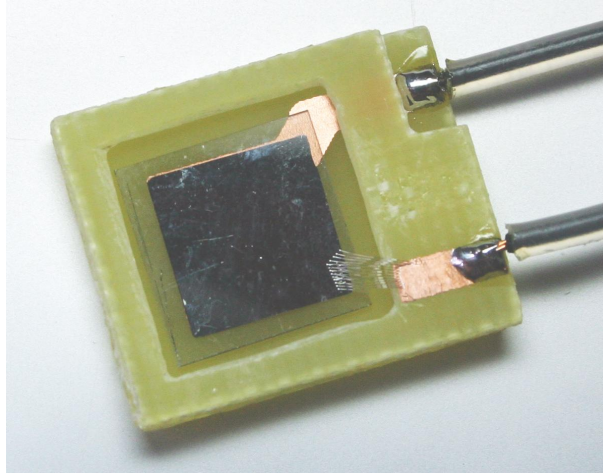


Figure 28: Photograph of the CDF diamond beam monitor package.

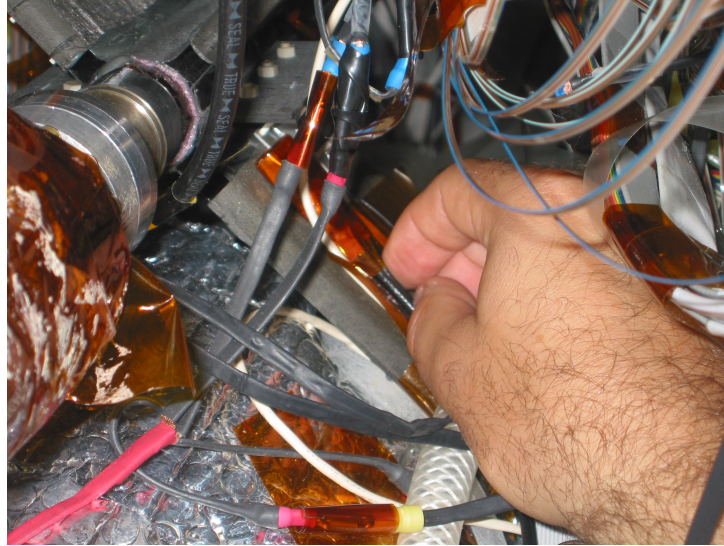


Figure 29: Photograph of the installation of the CDF diamond beam monitor.

In Fig. 30 we show the diamond response to the first beams at CDF. One observes that the diamond current is very small (pA) with no beams in the Tevatron (before 19:54) and generally follows the structure of the proton beam. The diamond monitor should be more correlated with the anti-proton beam but that data was not available. The instantaneous peaks of the order of 65 nA are easy to follow. CDF estimates that their signal to noise is between 100:1 and 1000:1. They are so pleased with the operation of the diamond that they have asked RD42 for additional diamonds.

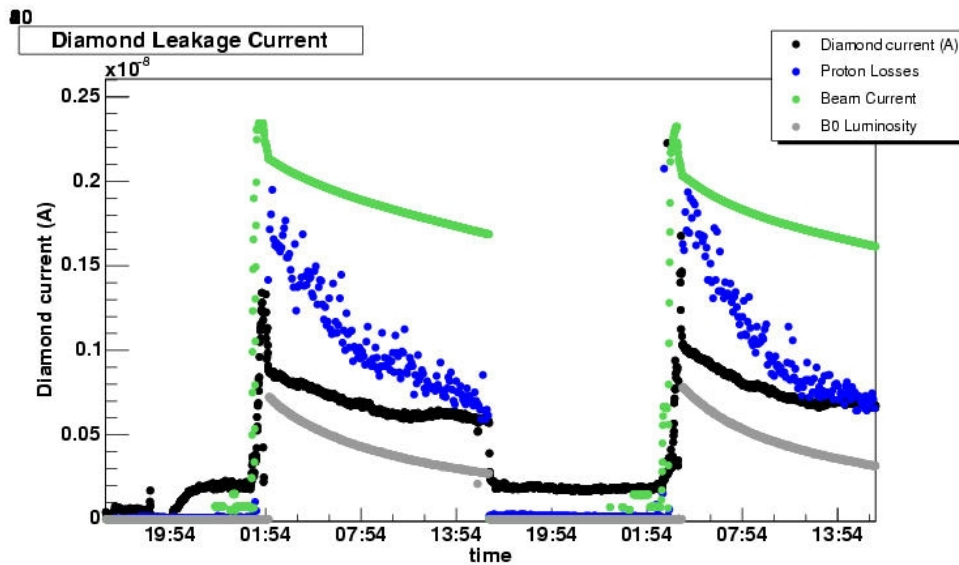


Figure 30: The operation of the CDF diamond beam monitor. The proton beam current is the upper trace (green); the measured proton beam loss is the second curve (blue); the diamond current is the third curve (black); the luminosity is the bottom curve (gray). One can see the turn on of the Tevatron at 19:54 and the residual beam current between fills.

The BaBar Diamond Radiation Monitor Program:

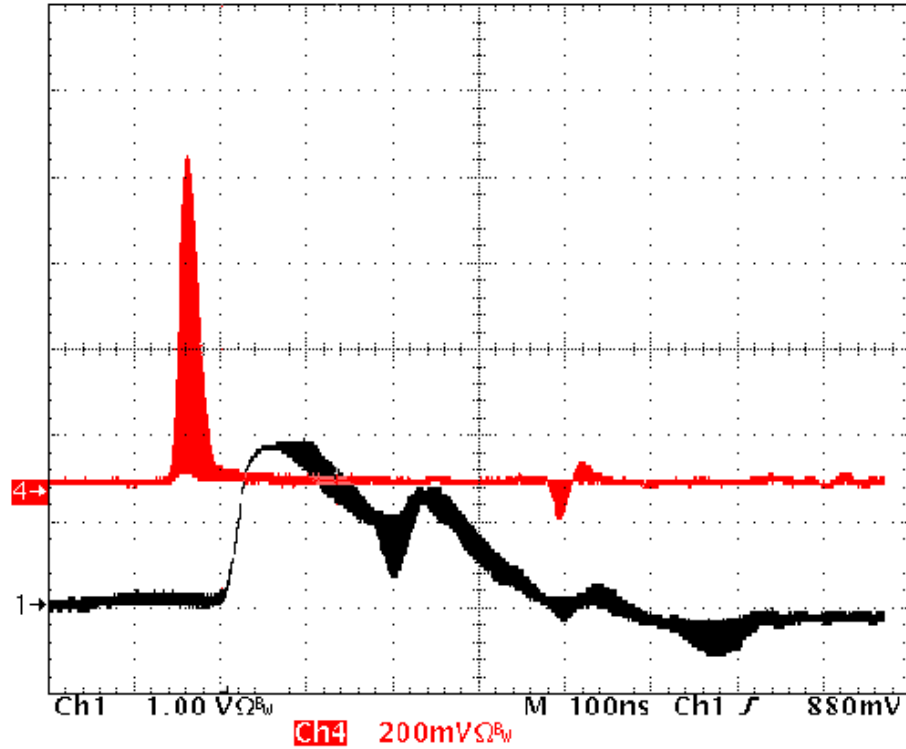


Figure 31: Data with pCVD diamond taken with a fast amplifier in BaBar. The upper plot shows the diamond current versus time. The second plot shows the SVTRad silicon photodiode during the same time period. These plots are triggered on the silicon PIN diode.

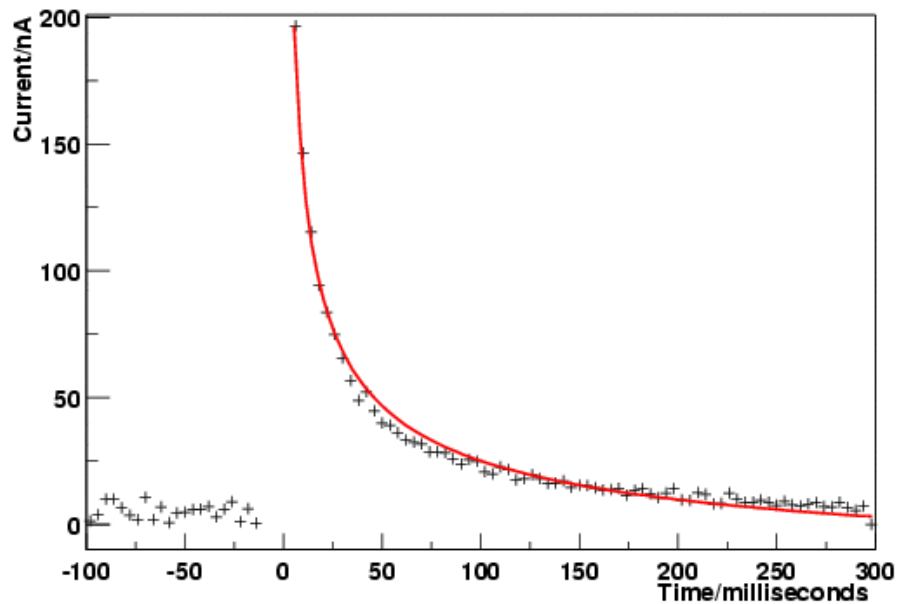


Figure 32: Expanded view of a beam loss event at the millisecond timescale in BaBar showing a clear tail. The tail is fit with a $1/\sqrt{t}$ function

Source Measurements and Erratic Dark Currents

- Estimate signal size $\sim 211\text{pA}$
- Source rate 170kHz , 1.6 cm from diamond, $\text{ccd}=215\ \mu\text{m}$
- $I = 170000 \cdot 215\ \mu\text{m} \cdot 36e/\mu\text{m} \cdot 1.6 \cdot 10^{-19}\text{C}/e = 211\text{pA}$

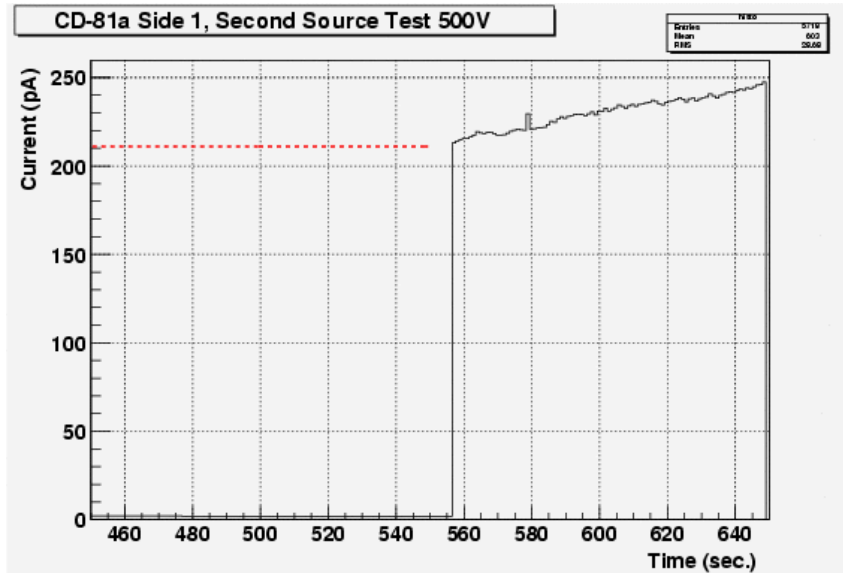


Figure 33: The current signal after addition of a ^{90}Sr source.

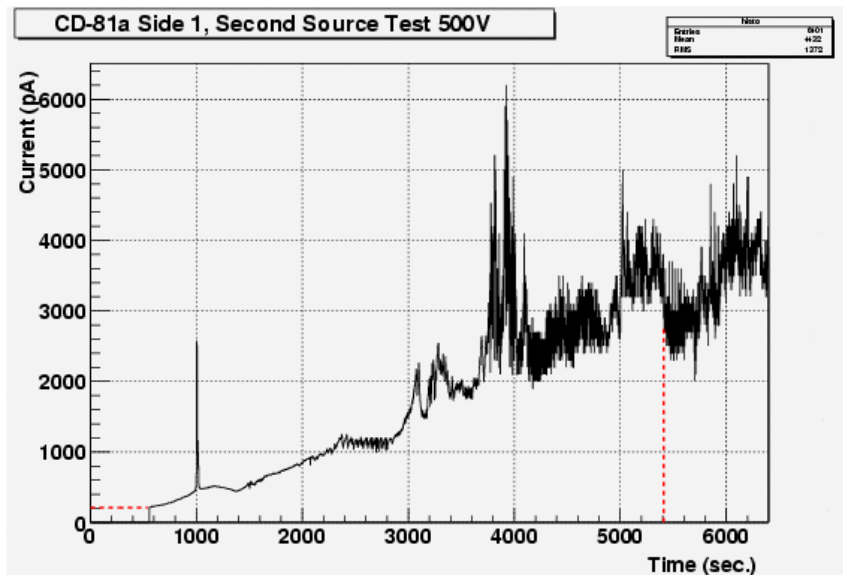


Figure 34: First few hours after addition of the source indicating the signal step and onset of erratic dark currents. After heating to 400°C for 4 minutes the extraneous currents are gone.

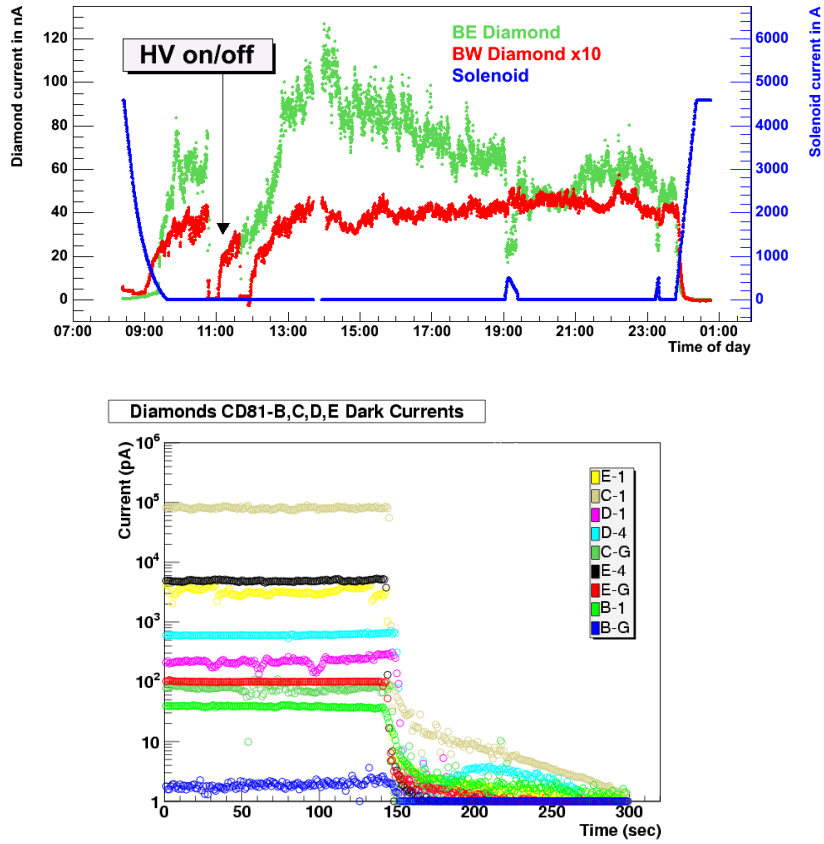


Figure 35: The discovery of erratic dark currents and the magnetic field suppression effect.

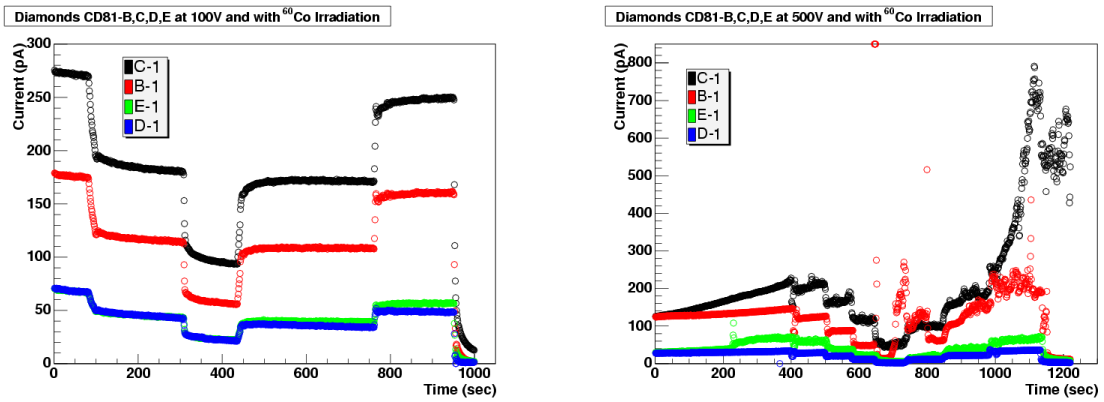


Figure 36: The high voltage suppression effect: left 100V, right 500V

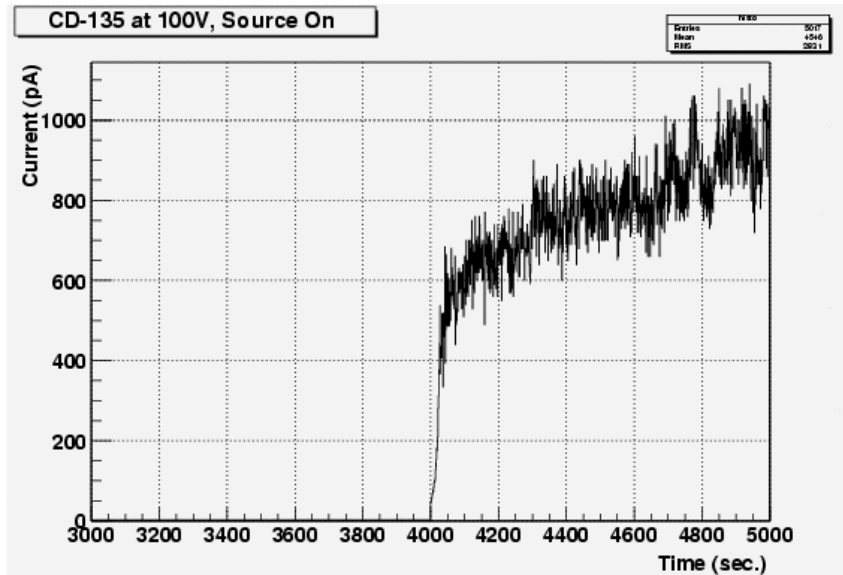


Figure 37: CD135 after irradiation with ^{60}Co , tested with ^{90}Sr . The signal is the small step. After a short time the diamond becomes unstable drawing approximately 1nA.

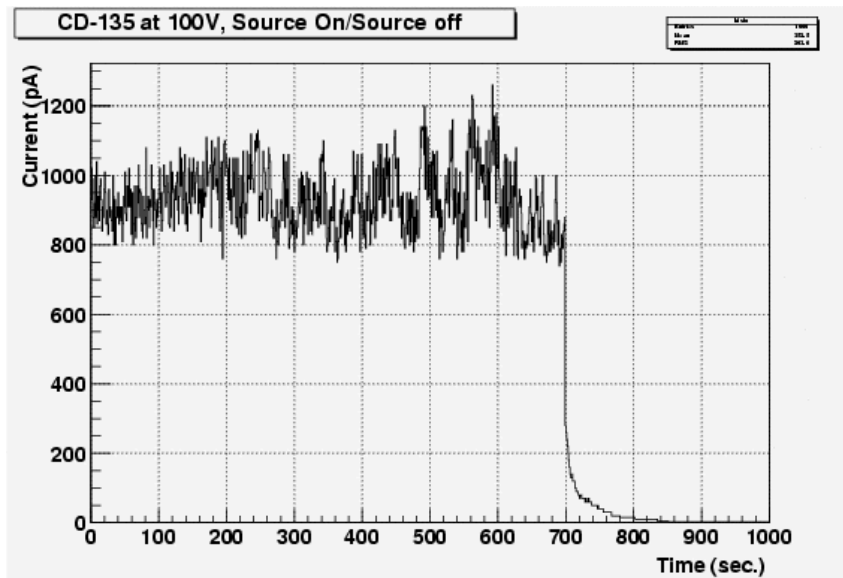


Figure 38: With the removal of the source shows that the unstable current disappears.

Final BaBar Package

- Ceramic package for rigidity and HV
- Mechanical constraints 2.3 mm height; 11 mm width; 13 mm length
- Leads out the end not top or bottom

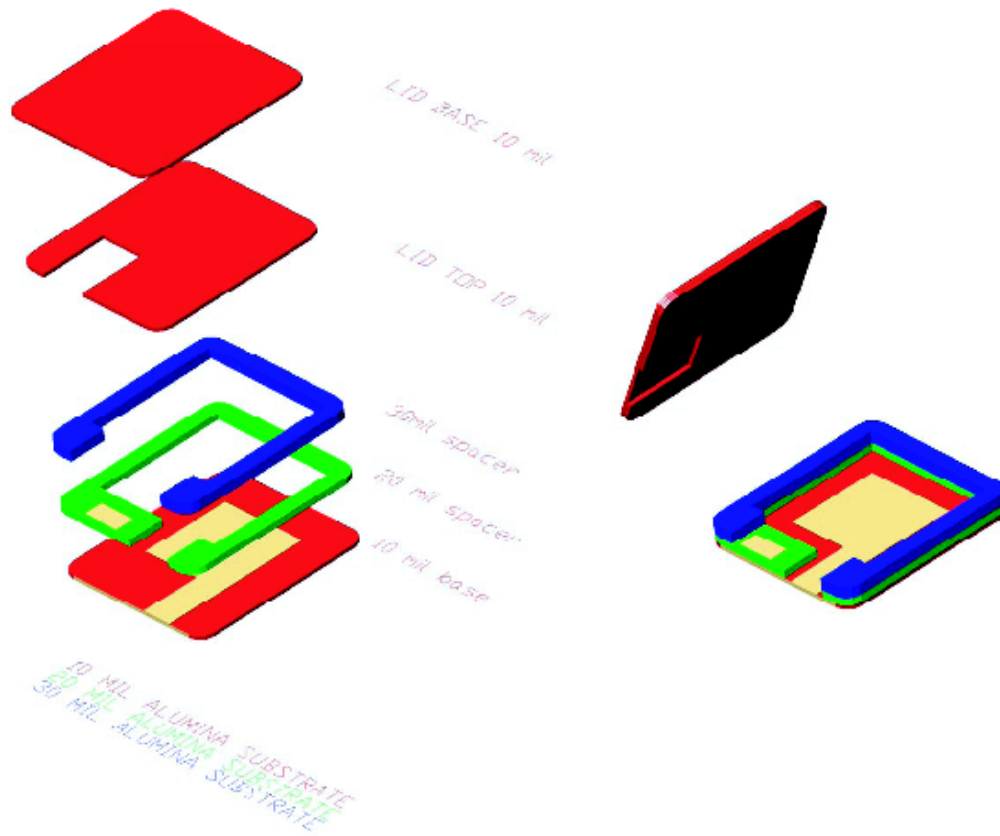


Figure 39: Cad drawing of the final BaBar package.

9 ATLAS Diamond Pixel Status:

Status:

- 3 1cm×1cm parts processed into pixel detectors and sent to IZM
 - 1 part fails - chemical spill
 - 1 part bump-bonded and performs poorly - suspect residual Ti/W above two parts re-processed and returned to IZM
 - two parts bump-bonded with FE-I3
 - two parts in ATLAS testbeam 2004!
- 1 2cm×6cm part processed into practice module and sent to IZM
 - practice module mounted in AlN wafer
 - questions of coating on surface
 - find no surface contaminants
 - problem is surface quality
 - practice module removed from AlN wafer by IZM and sent to E6 for re-processing
 - practice module sent from E6 to Toronto to OSU
 - practice module re-processed into pixel detector and sent to IZM
 - re-processed practice module bump-bonded with NO resistive shorts
- 1 2cm×6cm part processed into FINAL ATLAS module and sent to IZM
 - photo-lithography look ok
 - final module mounted in AlN wafer
 - final module being bump-bonded for ATLAS test beam in November
- 1 2cm×6cm bump-bonded at IZM and sent to Bonn for testing
 - module mounted according to ATLAS specs
 - all chips give signal with source
 - tested in ATLAS test beam in November

Detail of the Atlas Practice Module:

- we measured the roughness of the practice piece and found:
 - practice piece - Ra = 192 nm
 - 1cm × 1cm part - Ra = 5 nm
 - Al₂O₃ thin film ceramic - Ra < 130 nm

The roughness of the practice piece is worse than the roughness of commercial thin film ceramic. This makes the bump bonding very difficult. We need to apply a specification that the surface roughness in the final module will have Ra < 100 nm.

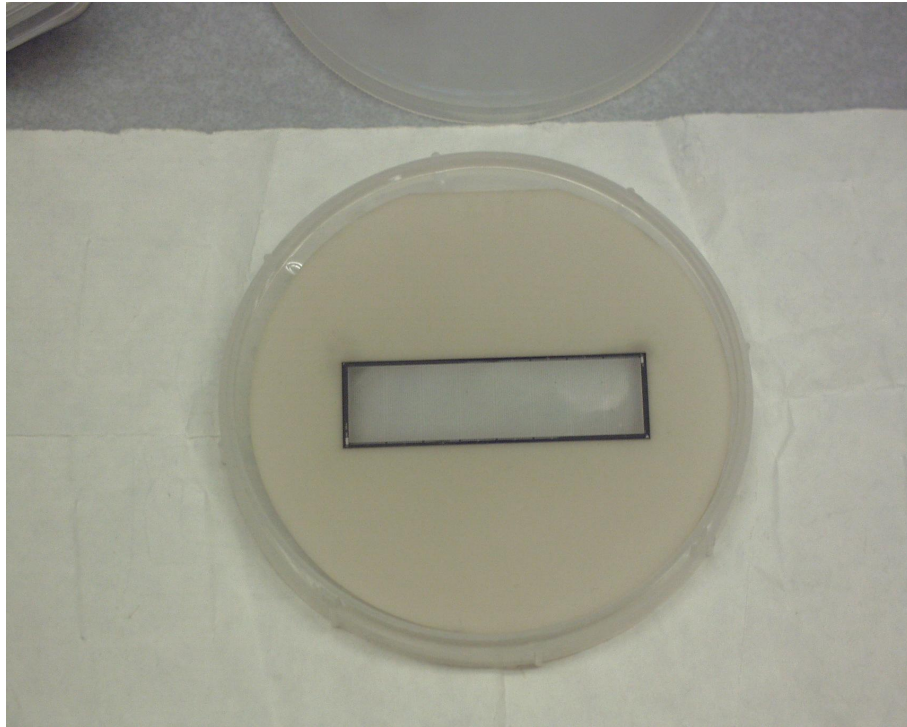


Figure 40: Photo of the front side of the Atlas pixel practice module illustrating the surface quality.

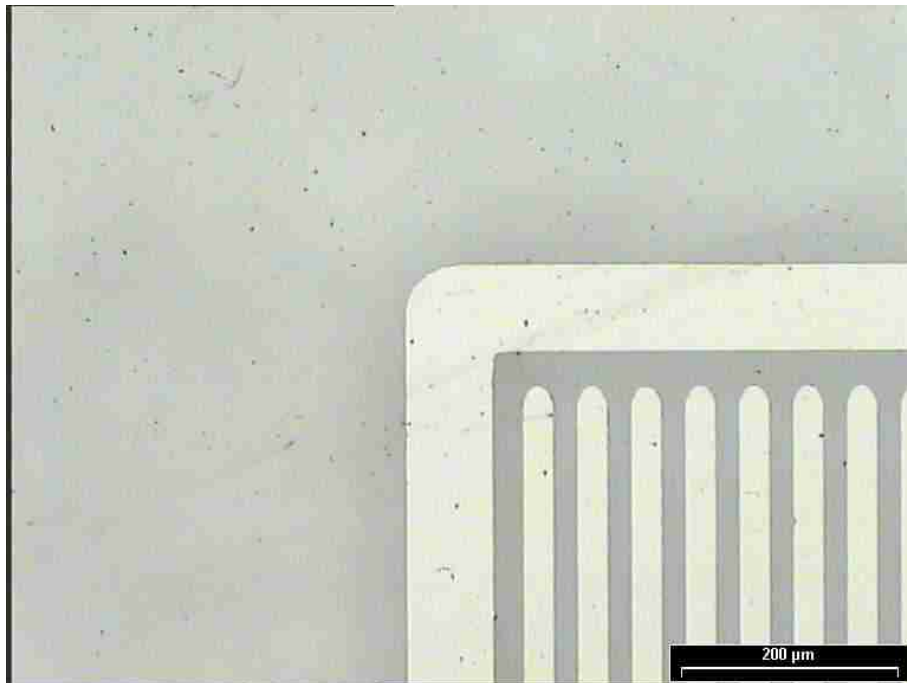


Figure 41: The surface of an ATLAS 1cm x 1cm pixel detector. The magnification is 100x.

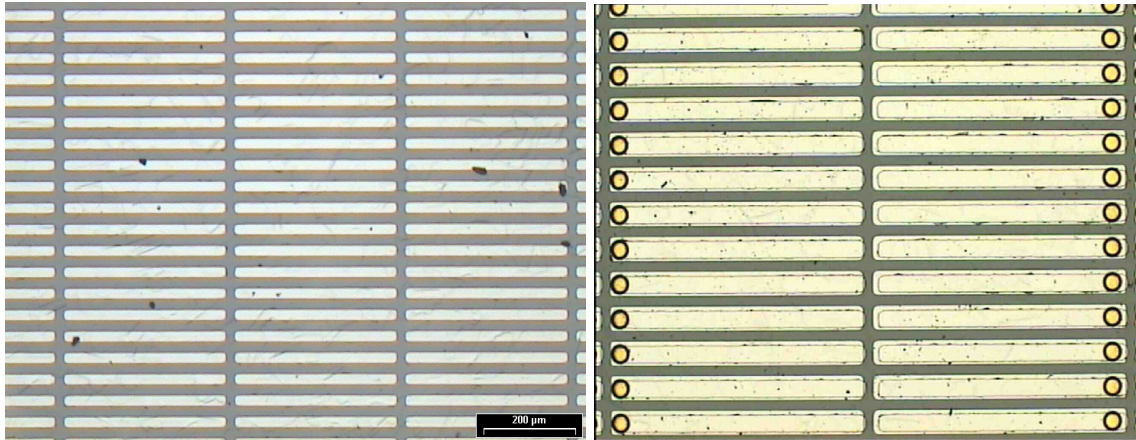


Figure 42: Photograph of the pixel pattern on the final ATLAS pixel module before and after the under-bump metal is deposited.

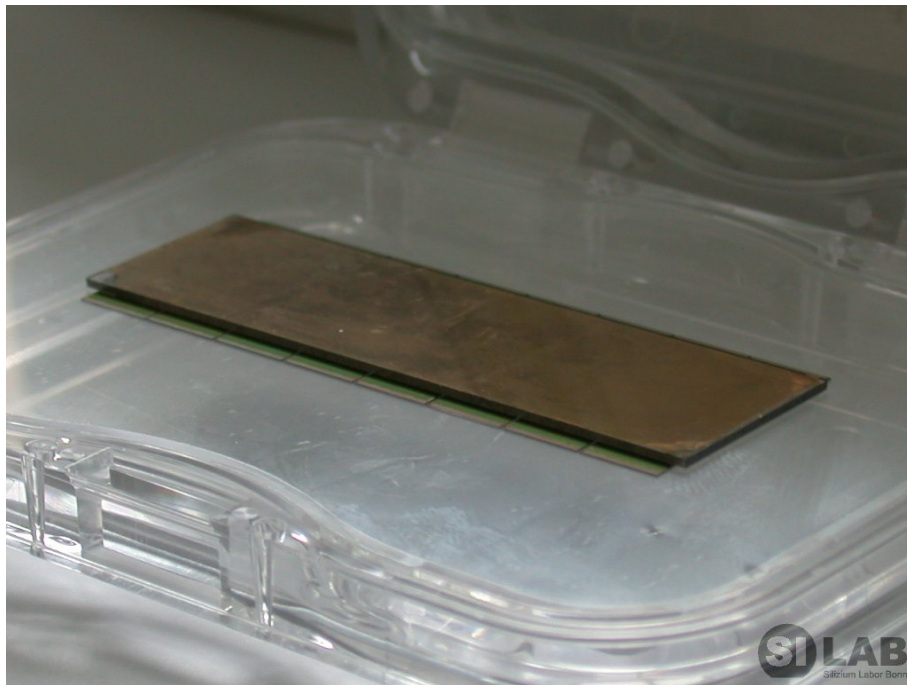


Figure 43: Final ATLAS pixel module with electronics mounted.

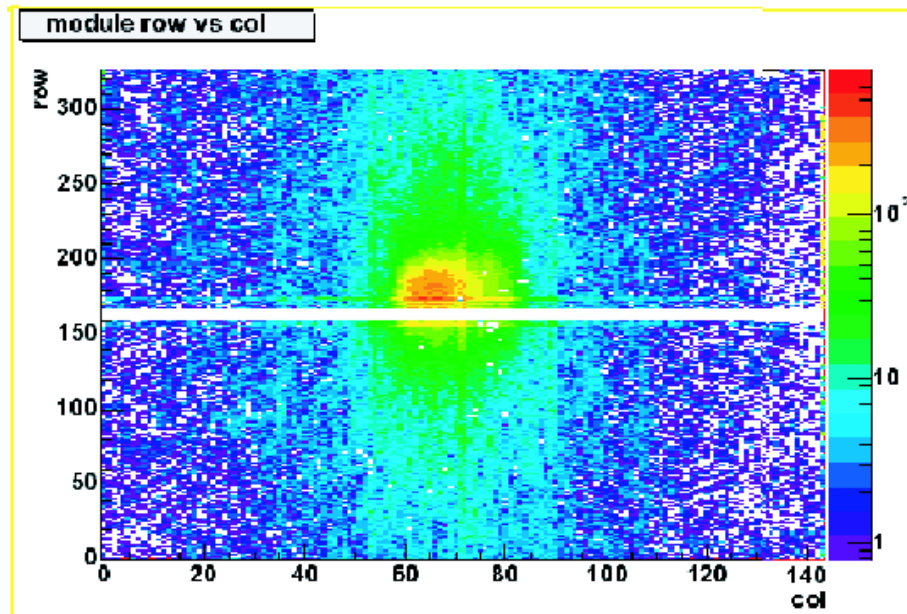


Figure 44: First ATLAS pixel module results.

10 Wafer Measurements and Processing:

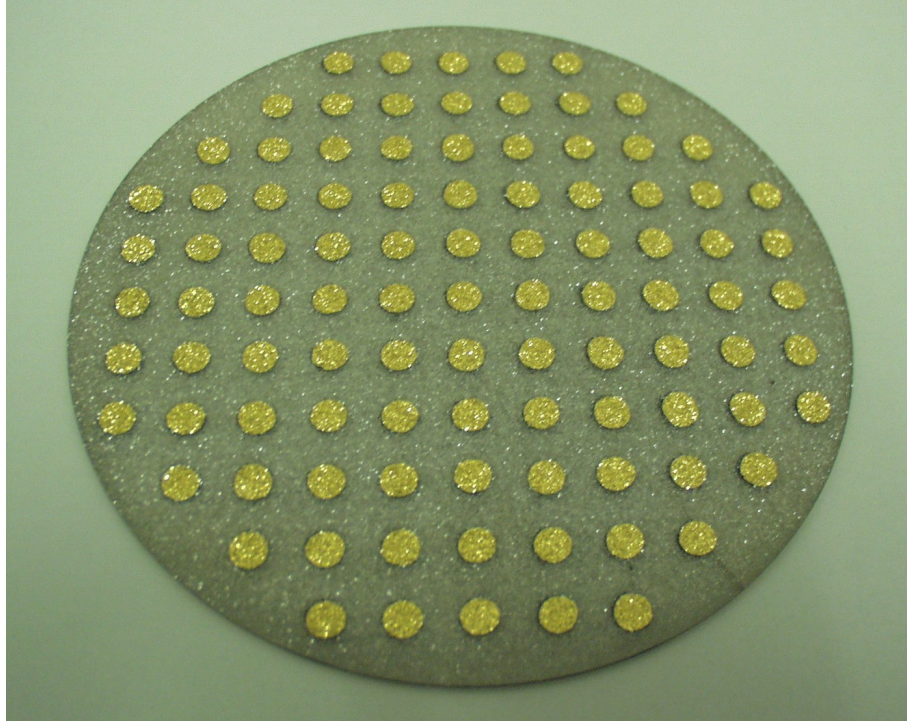


Figure 45: Photo of the growth side of the wafer metalised for testing.

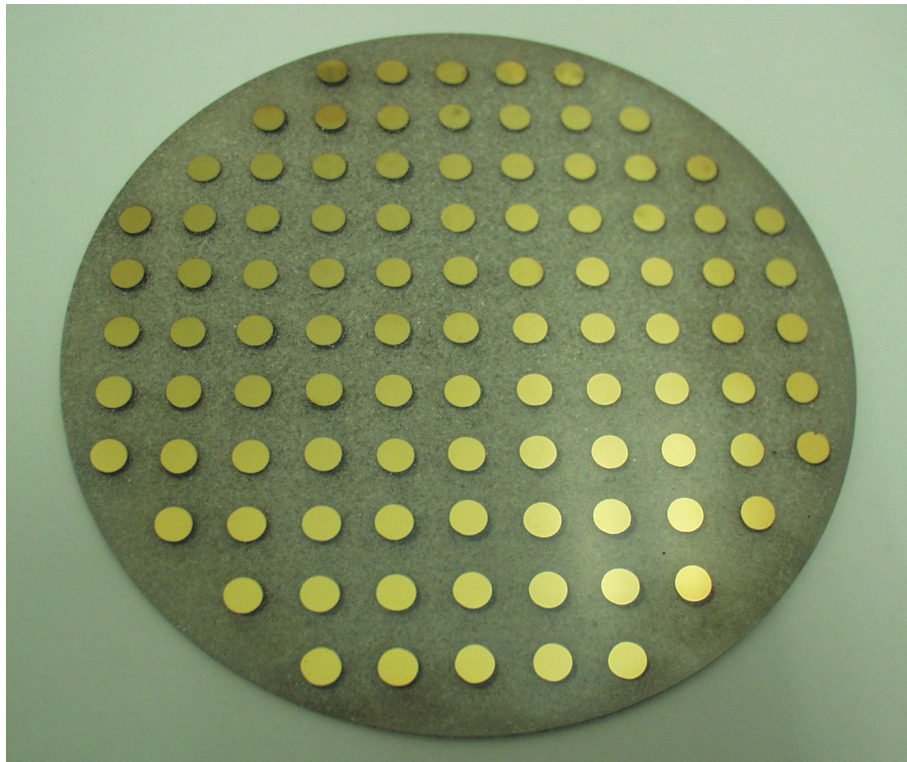


Figure 46: Photo of the substrate side of the wafer metalised for testing.

Wafer measurements were performed on the grid shown above. A total of 96 points were measured. Below is the charge collected versus high voltage for (0,1).

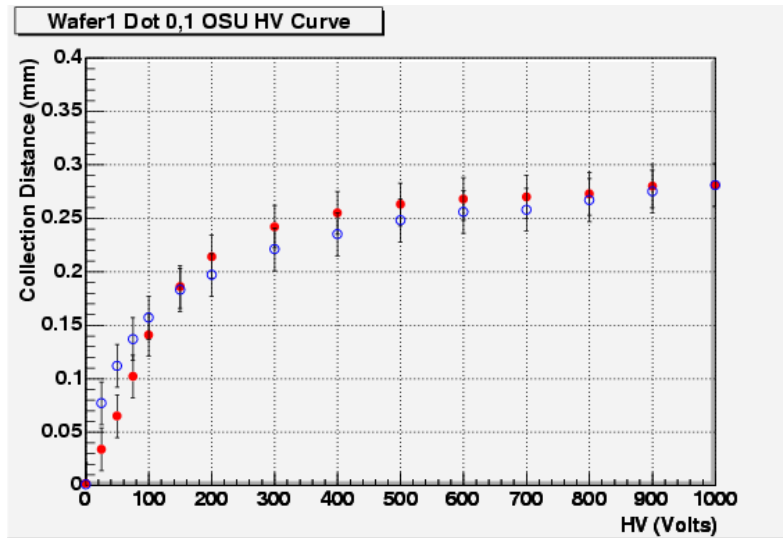


Figure 47: Collection distance for wafer point (0,1). The thickness of the diamond at (0,1) is 1390 μm .

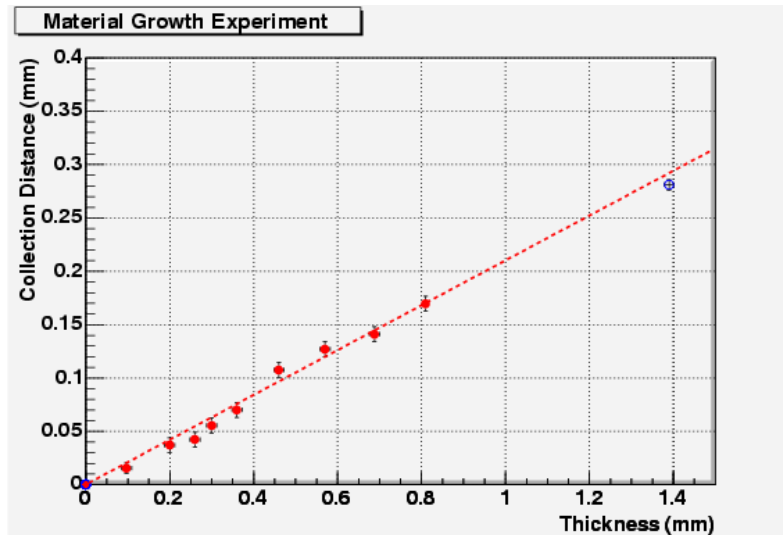


Figure 48: Plot of collection distance for wafer point (0,1) overlaid with the thinning experiment data.

Thickness Map

	-5	-4	-3	-2	-1	0	1	2	3	4	5
5				1.15	1.18	1.16	1.16	1.16			
4			1.18	1.18	1.18	1.18	1.18	1.18	1.14		
3		1.16	1.19	1.22	1.27	1.28	1.24	1.19	1.17	1.15	
2	1.17	1.20	1.21	1.26	1.31	1.31	1.30	1.24	1.18	1.18	1.18
1	1.17	1.19	1.21	1.30	1.34	1.39	1.36	1.30	1.21	1.21	1.18
0	1.15	1.15	1.22	1.28	1.35	1.39	1.33	1.30	1.22	1.19	1.17
-1	1.15	1.16	1.19	1.25	1.31	1.32	1.27	1.25	1.20	1.15	1.17
-2	1.09	1.09	1.13	1.16	1.25	1.25	1.24	1.18	1.15	1.14	1.15
-3		1.09	1.12	1.12	1.13	1.17	1.14	1.10	1.06	1.06	
-4			1.07	1.05	1.06	1.04	1.03	1.03	1.05		
-5				1.03	1.02	1.04	1.04	1.05			

 Marks the crack

Figure 49: Plot of thickness as a function of position for wafer 1.

Collection Distance

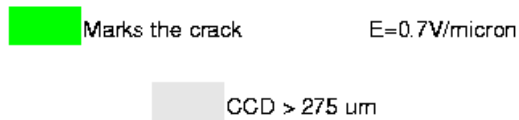
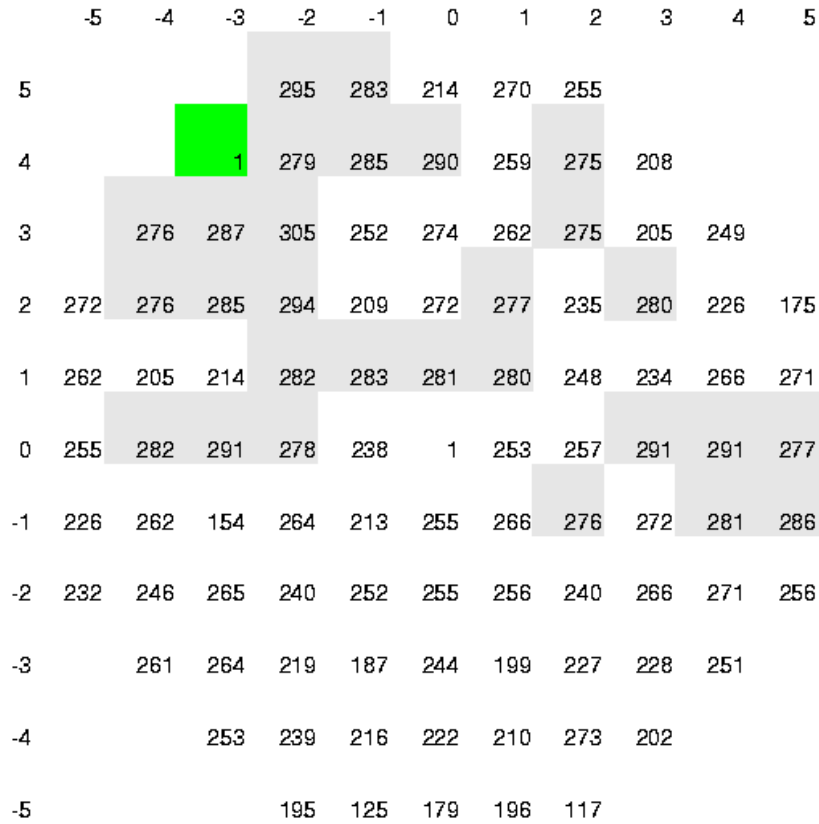


Figure 50: Plot of collection distance as a function of position for wafer 1. The grey areas represent regions where the collection distance is greater than 275 μm . The lower half of the wafer is clearly inferior to the upper half.

The collection distance measurements of seven diamonds from the wafer are shown below:

 Comparison of E6-Wafer1 Measurements Before and After Processing

Notes: All diamonds measured at HV=600V (Before, CD165 HV=1000V)

pd1 -> pumps down side 1

pu1 -> pumps up side 1

np1 -> no pumping on side 1

Name	Location	t	ccd	t'	Offset	ccd'	
CD144	-1.5, 3.0	1250	276	515	7-10	228/199	- pd1; np2
144m					13-19	218/199	- np1; np2 *
CD145	-.75, 3.0	1280	260	515	7-1	230->221/208	- pd1; np2
145r				490	2-4	226/209	- np1; np2
CD146	.25, 3.0	1270	270	515	12-22	225/221->209	- np1; pd2 *
146r				490	3-5	208/210	- np1; np2
CD147	1.2, 3.0	1230	265		11-14	251/221	- np1; pu2
CD148	2.0, 3.0	1190	275	535	7-12	225/224	- pd1; np2
CD157				480	2-7	214->211/202->215	- pd1; pu2
CD158r				490	1-5	213/201	- np1; np2
CD159	3.75, 1.75	1190	230		10-19	197/195	- np1;
159m							
159m'		1190	230		6	187/	-
CD160	3.75, 0.75	1200	246		12-17	183/170	- pd1; pu2
160m							
160m'		1200	246		6	153	-
CD165	0.0,0.0	1390	257	1180	1-10	234/229	- pu1; pu2 *
-----Control Samples-----							
UT14-2				555	3-9	182/170	- pu1; pu2 *
UT14-3				550	1-3	183/	
-----Plasma Samples-----							
UT13-1				615	2	181-190/178-181	- pu1; pu2
UT13-4				615	2	169-196/197-198	- pu1; p

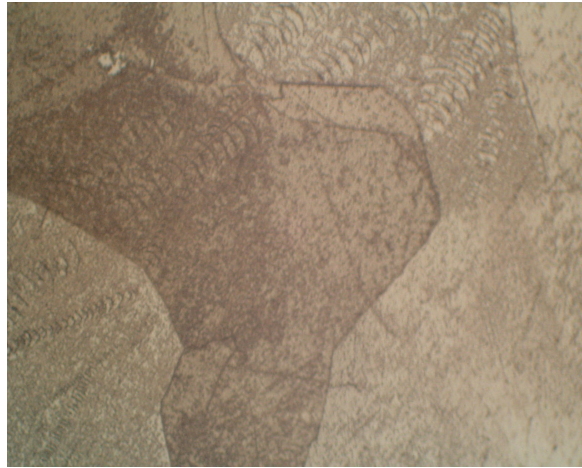


Figure 51: Photographs of UT13-4 middle, corner side 1 and corner side 2.